Numerical General Relativity in the Context of the Hadron-Quark Phase Transition in Compact Stars

Physics Theory Palaver   Johann Wolfgang Goethe-University   January 26, 2015

Matthias Hanauske

Johann Wolfgang Goethe-University
Institute for Theoretical Physics
Department of Relativistic Astrophysics
*Max-von-Laue-Str. 1*
D-60438 Frankfurt am Main
Germany

Numerical General Relativity in the context of the Hadron-Quark Phase Transition in Compact Stars

1. Introduction

2. The Hadron-Quark Phase Transition in the Interior of Compact Stars

3. Neutron Stars, Hybrid Stars and Quark Stars

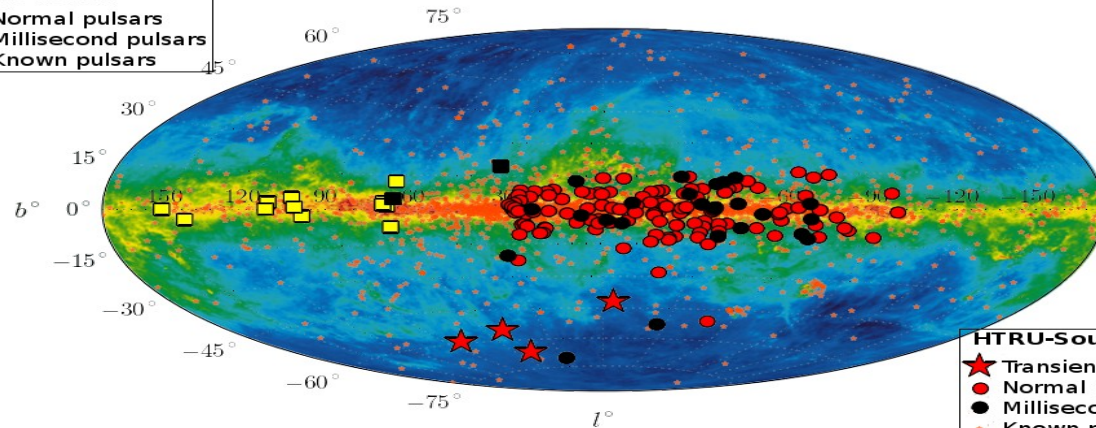4. Numerical General Relativity and Relativistic Hydrodynamics
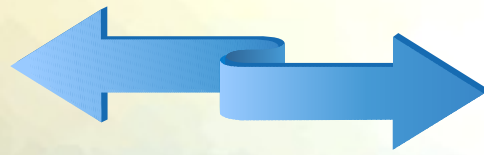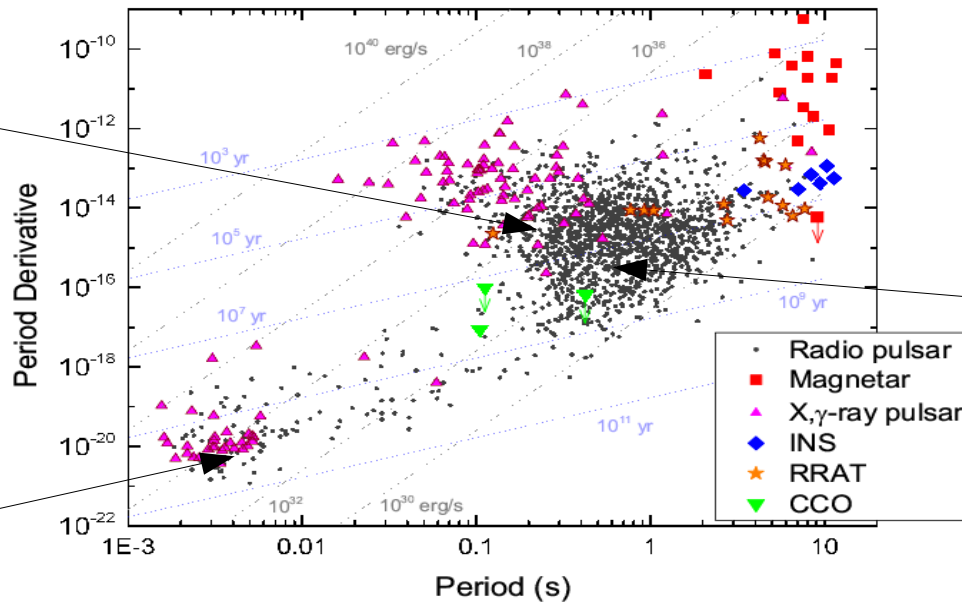
Pulsars ⟷ Compact Stars
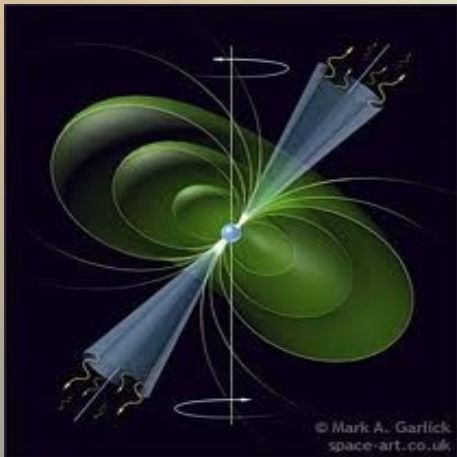
HTRU-North:
- ☐ Normal pulsars
- ■ Millisecond pulsars
- ✱ Known pulsars

HTRU-South:
- ★ Transient bursts
- ● Normal pulsars
- ● Millisecond pulsars
- ✱ Known pulsars

PSR B0531+21 (33.5 ms)
Crab Pulsar

PSR B0329+54 (0.715 s)

PSR B1937+21 (1.56 ms)

- • Radio pulsar
- ■ Magnetar
- ▲ X,γ-ray pulsar
- ◆ INS
- ★ RRAT
- ▼ CCO

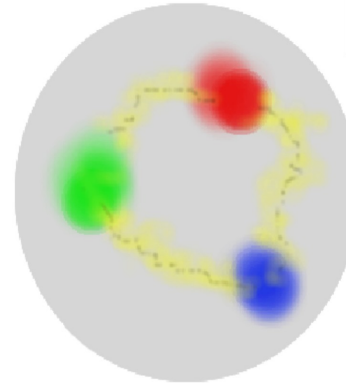# General Relativity and Quantum Cromodynamics

	ART	Yang-Mills-Theories
	$D_\beta v^\alpha = \partial_\beta v^\alpha + \Gamma^\alpha_{\sigma\beta} v^\sigma$	$D_{\beta a}{}^b = \partial_\beta 1_a{}^b + ig\, A_{\beta a}{}^b$
	$R^\delta{}_{\mu\alpha\beta} v^\mu = [D_\alpha, D_\beta] v^\delta$	$F_{\alpha\beta a}{}^b = \frac{1}{ig}\left[D_{\alpha a}{}^c, D_{\beta c}{}^b\right]$
	$R^\delta{}_{\mu\alpha\beta} = \Gamma^\delta_{\mu\alpha|\beta} - \Gamma^\delta_{\mu\beta|\alpha}$	$= A_{\beta a}{}^b{}_{|\alpha} - A_{\alpha a}{}^b{}_{|\beta}$
	$+\Gamma^\delta_{\nu\beta}\Gamma^\nu_{\mu\alpha} + \Gamma^\delta_{\nu\alpha}\Gamma^\nu_{\mu\beta}$	$+\frac{1}{ig}\left[A_{\alpha a}{}^c, A_{\beta c}{}^b\right]$
	$\mathcal{L}_G = R + \underbrace{(c_1 R_{\mu\nu}R^{\mu\nu} + ...)}_{\equiv 0 \text{ for ART}}$	$\mathcal{L}_{YM} = \frac{1}{4}F_{\mu\nu a}{}^b\, F^{\mu\nu}{}_a{}^b$

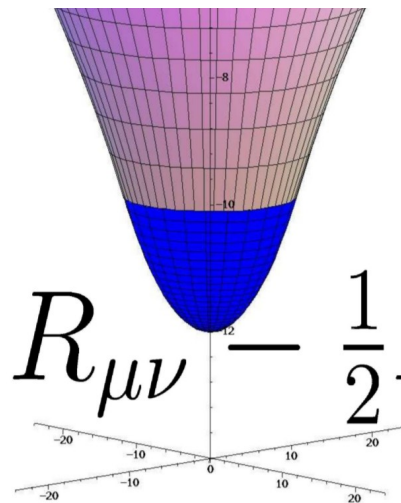QuantumCromoDynamic:

$(SU(3)_{(c)}$- Color Yang-Mills-Gauge Theory)

$D_{\beta A}{}^B = \partial_\beta 1_A{}^B + ig\, G_{\beta A}{}^B$

$A,{}^B$ =red, green, blue

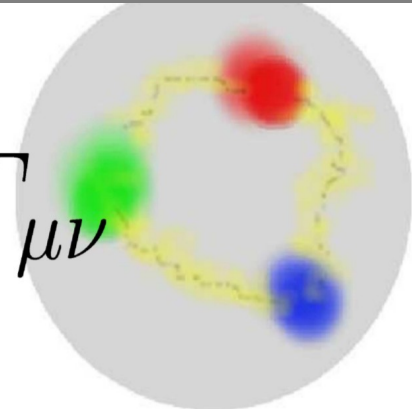$\psi_A^f = \begin{pmatrix} \psi_r^f \\ \psi_g^f \\ \psi_b^f \end{pmatrix}$

Confinement
chiral symmetry, ...

$$R_{\mu\nu} - \frac{1}{2} R\, g_{\mu\nu} = \frac{8\pi G}{c^4}\, T_{\mu\nu}$$

Numerical General Relativity in the context of the Hadron-Quark Phase Transition in Compact Stars

The QCD- Phase Diagram I

The QCD phase diagram at temperature T and net baryon density is displayed on the right side.

Some regions can be accessed by heavy ion collisions at different energies.

Matter of the early universe and in the interior of compact stars are also indicated within the diagram.
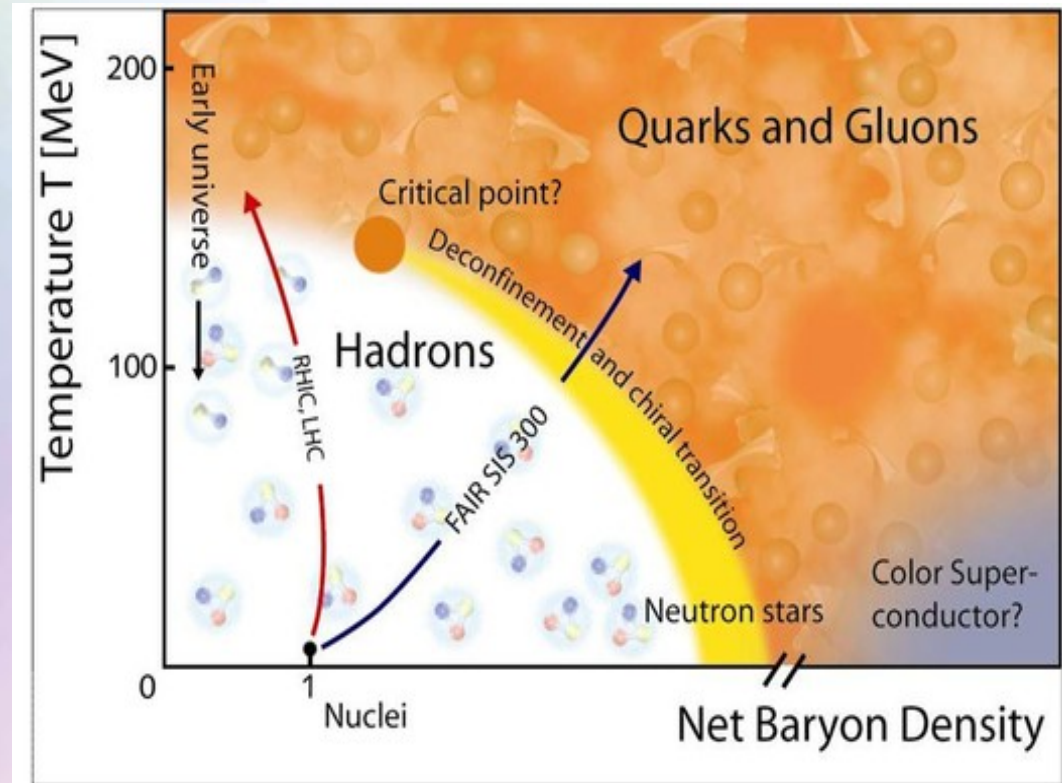

Image from
http://webarchiv.fz-juelich.de/nic/Publikationen/Broschuere/
Elementarteilchenphysik/hadron.jpg
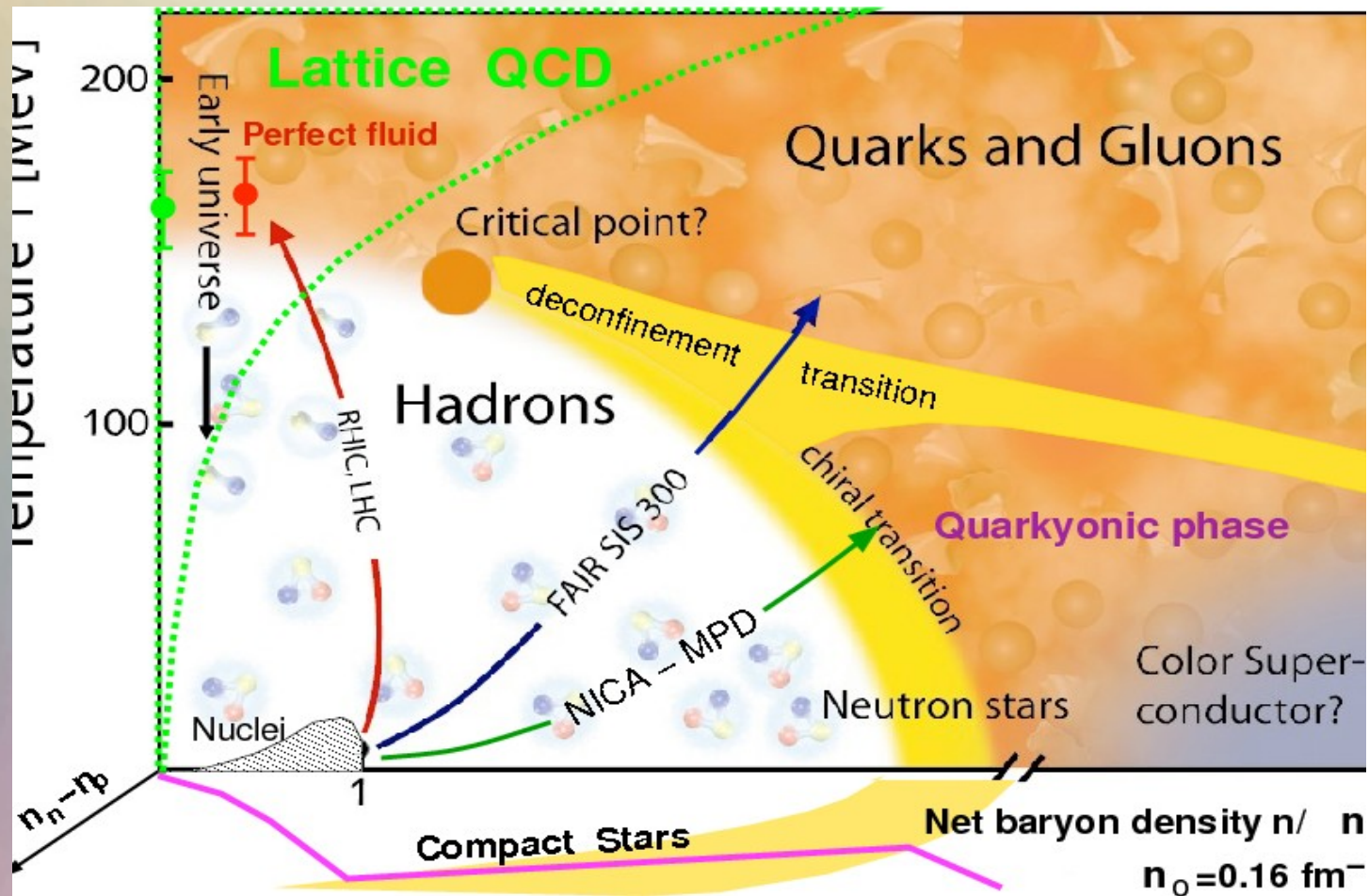
The QCD- Phase Diagram II

Image from http://inspirehep.net/record/823172/files/phd_qgp3D_quarkyonic2.png

The QCD – Phase Transition

The appearance of the QCD - phase transition (the transition from confined hadronic to deconfined quark matter) will change the properties of neutron stars. Whether this change will be visible with telescopes and gravitational wave antennas depends strongly on the equation of state of hadronic and quark matter and on the construction of the phase transition.
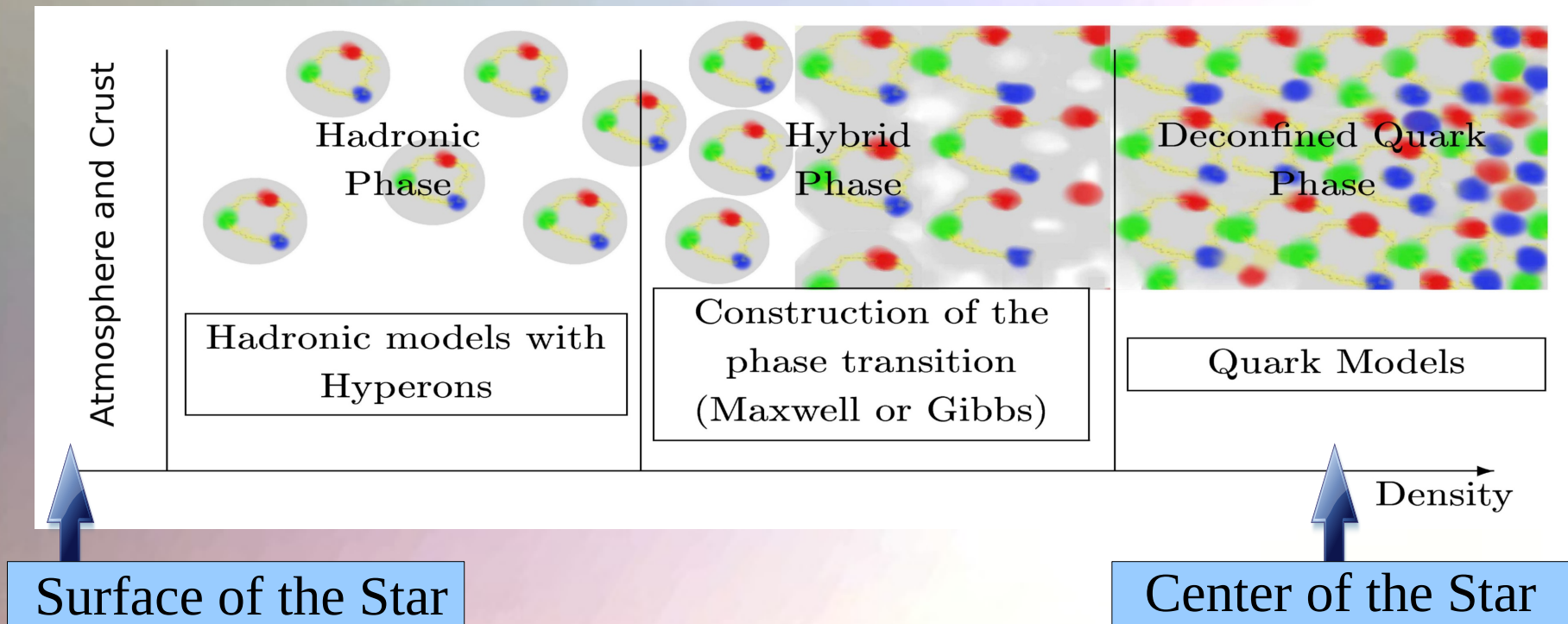
Numerical General Relativity in the context of the Hadron-Quark Phase Transition in Compact Stars

1. Introduction
2. The Hadron-Quark Phase Transition in the Interior of Compact Stars
3. **Neutron Stars, Hybrid Stars and Quark Stars**
4. Numerical General Relativity and Relativistic Hydrodynamics

The Compact Star Zoo

Depending on the model used, the compact star zoo consists of different inhabitants: e.g. neutron stars with and without hyperons, quark stars and strange quark stars, hybrid stars with color superconducting quark matter, hybrid stars with Bose-Einstein condensates of antikaons.
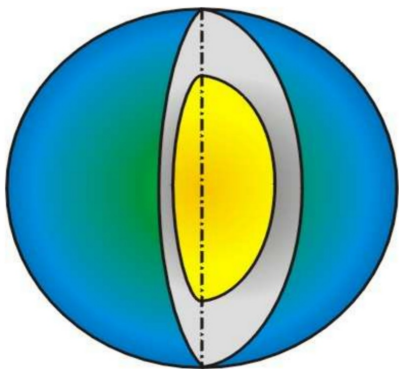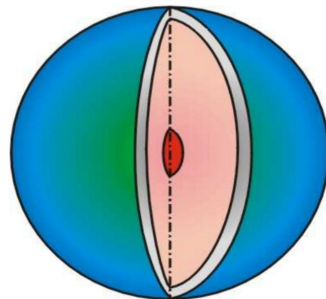
Neutron Stars   Hybrid Stars   Quark Stars   Black Holes

$\rho_c = \rho_0$ $\approx 2\,\rho_0$ $\approx 5\,\rho_0$ $\ldots \infty$

Central density ρ_c in the star

$(\rho_0 := 0.15/\mathrm{fm}^3)$

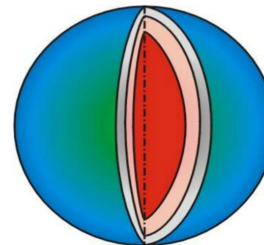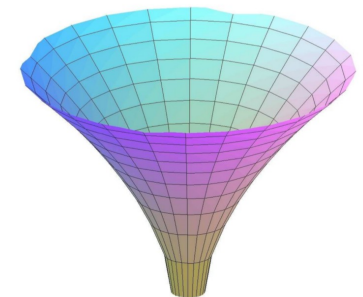# Neutron Stars

(Simplest model: Nonrotating, sperical symmetric, static, ideal fluid)

$$T^{\mu\nu} = (\epsilon + p)u^{\mu}u^{\nu} + pg^{\mu\nu}$$

$$R_{\mu\nu} - \frac{1}{2}R\,g_{\mu\nu} \;=\; \frac{8\pi G}{c^4}\;T_{\mu\nu}$$

Tolman-Oppenheimer-Volkoff Equation

$$\frac{dP}{dr} \;=\; -\frac{(\epsilon + P)4\pi r^3 + m}{r(r - 2\,m)}$$
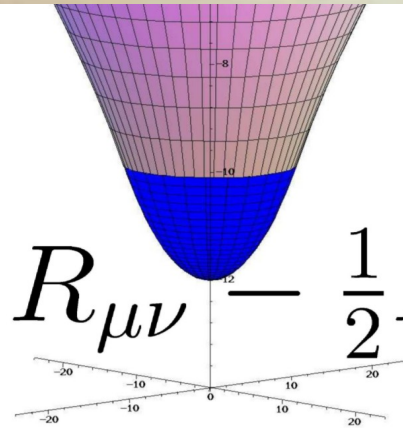
$$m(r) \;=\; \int_0^r 4\pi \tilde{r}^2 \epsilon(\tilde{r})\;d\tilde{r}$$
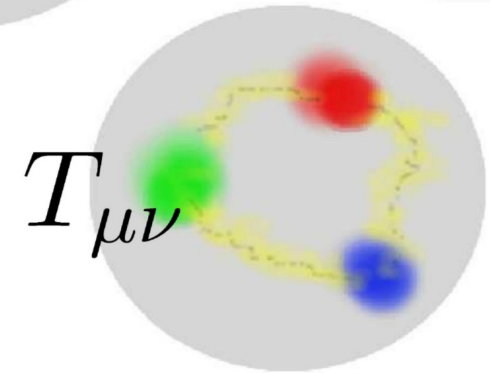
$$\frac{d\nu}{dr} \;=\; \frac{8\pi P r^3 + 2\,m}{r(r - 2\,m)}\quad,$$

Space-Time Metric :

$$g_{\mu\nu} \;=\; \begin{pmatrix} e^{\nu(r)} & 0 & 0 & 0 \\ 0 & -\left(1 - \frac{2\,m(r)}{r}\right)^{-1} & 0 & 0 \\ 0 & 0 & -r^2 & 0 \\ 0 & 0 & 0 & -r^2\sin^2\theta \end{pmatrix}$$

Neutron Stars (NS)

$$R_{\mu\nu} - \frac{1}{2} R \, g_{\mu\nu} \;=\; \frac{8\pi G}{c^4} \, T_{\mu\nu}$$

Relativistic Mean-Field Hadronic Models

$$\sum_B \; (p, n, \Lambda, \Sigma^-, \, \Sigma^0, \Sigma^+, \, \Xi^-, \Xi^0)$$
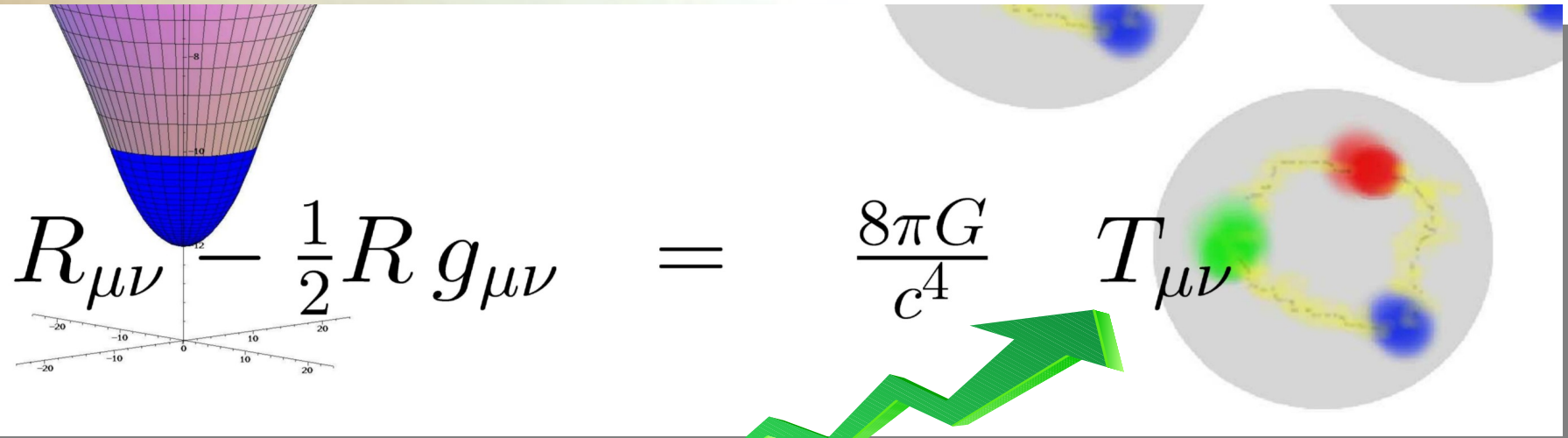
$$
\begin{aligned}
\mathcal{L} \;=\; & \sum_B \overline{\psi}_B \left(i\slashed{\partial} - m_B \right) \psi_B + \frac{1}{2}\partial^\mu \sigma \partial_\mu \sigma - \frac{1}{2}m_\sigma^2 \sigma^2 - \frac{a}{3}\sigma^3 - \frac{b}{4}\sigma^4 - \frac{1}{4}\omega^{\mu\nu}\omega_{\mu\nu} \\
& + \frac{1}{2}m_\omega^2 \omega^\mu \omega_\mu - \frac{1}{4}\vec{\rho}^{\,\mu\nu}\vec{\rho}_{\mu\nu} + \frac{1}{2}m_\rho^2 \vec{\rho}^{\,\mu}\vec{\rho}_\mu + \sum_B \overline{\psi}_B \left(g_{\sigma B}\sigma + g_{\omega B}\omega^\mu \gamma_\mu + g_\rho \vec{\rho}^{\,\mu}\gamma_\mu \vec{\tau}_B \right) \psi_B
\end{aligned}
$$

$$
\begin{aligned}
\mathcal{L}^{YY} \;=\; & \frac{1}{2}\left(\partial^\mu \sigma^* \partial_\mu \sigma^* - m_{\sigma^*}^2 \sigma^{*2} \right) - \frac{1}{4}\phi^{\mu\nu}\phi_{\mu\nu} + \frac{1}{2}m_\phi^2 \phi^\mu \phi_\mu \\
& + \sum_Y \overline{\psi}_Y \left(g_{\sigma^* Y}\sigma^* + g_{\phi Y}\phi^\mu \gamma_\mu \right) \psi_Y \quad,
\end{aligned}
$$

$$\mathcal{L}_{\text{lep}} \;=\; \sum_{l=e,\mu} \overline{\psi}_l [i\gamma_\mu \partial^\mu - m_l]\psi_l$$

Composition of Neutron Star Matter

Neutron star matter conditions:

1) Charge Neutrality
2) β-equilibrium
3) Strangeness production

Λ-Hyperon $\quad n + n \leftrightarrow n + \Lambda + K^0 \quad \mu_\Lambda = \mu_n$

Σ^--Hyperon $\quad n + n \leftrightarrow n + \Sigma^- + K^+ \quad \mu_{\Sigma^-} = \mu_n + \mu_e$

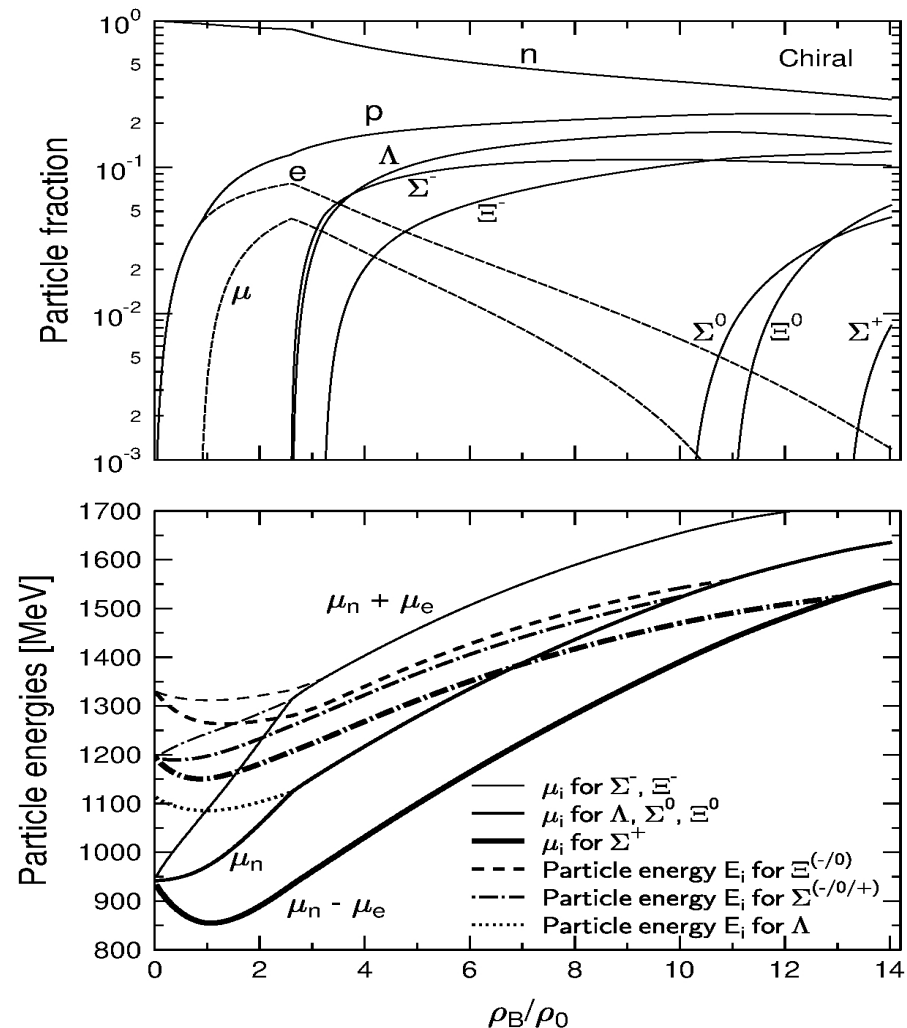Chemical potentials and single particle energies of hyperons in dependence of the baryonic density.

$$E_i(k) = E_i^*(k) + g_{i\omega}\omega_0 + g_{i\phi}\phi_0 + g_{i\rho}I_{3i}\rho_0$$

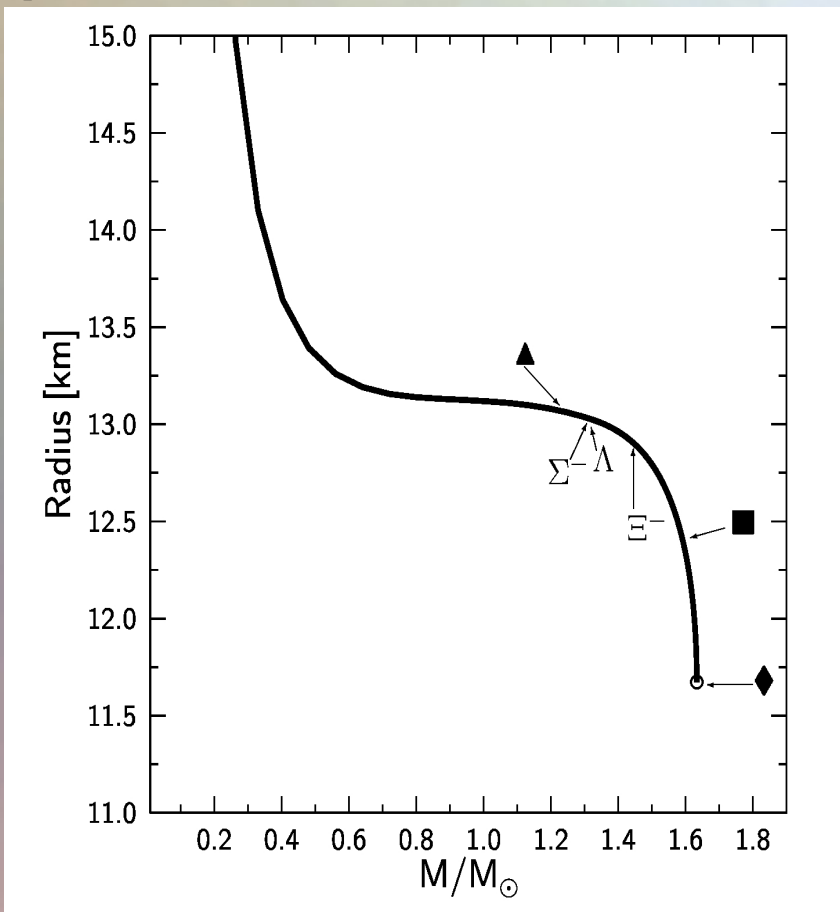$$E_i^*(k) = \sqrt{k_i^2 + m_i^{*2}} \qquad \mu_i = b_i\mu_n - q_i\mu_e$$

M. Hanauske, D. Zschiesche, S. Pal, S. Schramm, H. Stöcker, and W. Greiner, Astrophys. J. 537, 958 (2000)

Particle composition vs baryonic density

Neutron Star Properties

The neutron star radius as a function of its mass. A low, middle and high density star is displayed within the figure. Additionally the onset of hyperonic particles is visualized.

Energy density profiles of three neutron stars with different central densities and masses. The low density stars do not contain any hyperons, whereas the other two stars do have hyperons in their inner core.
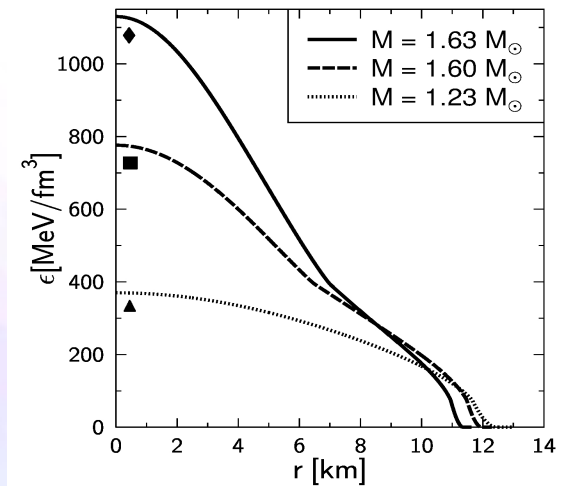
Time-time component of the metric tensor as a function of the radial coordinate. The solid line corresponds to the inner TOV-solution, whereas the doted curve depicts the outer Schwarzschild part.

Hybrid Stars

$$R_{\mu\nu} - \frac{1}{2} R\, g_{\mu\nu} \;=\; \frac{8\pi G}{c^4}\, T_{\mu\nu}$$
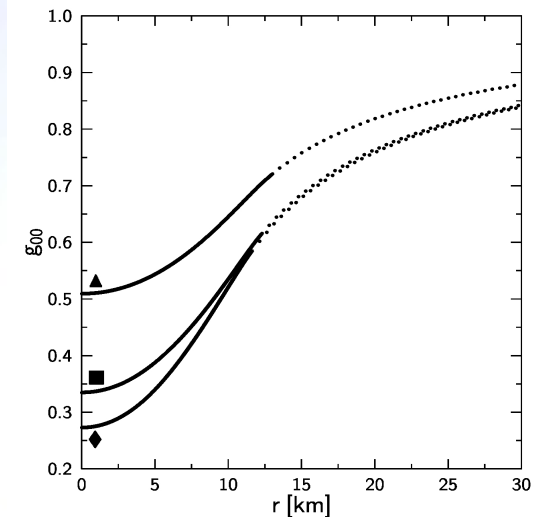
Hadronic Model + Quark Model (eg. NJL model or MIT-Bag model)

Lagrangian density of the NJL model

$$\mathcal{L} \;=\; \underbrace{\overline{\psi}\,(i\,\slashed{\partial} - \hat{m}_0)\,\psi}_{\text{Kinetische und Massenbeiträge}} \; \und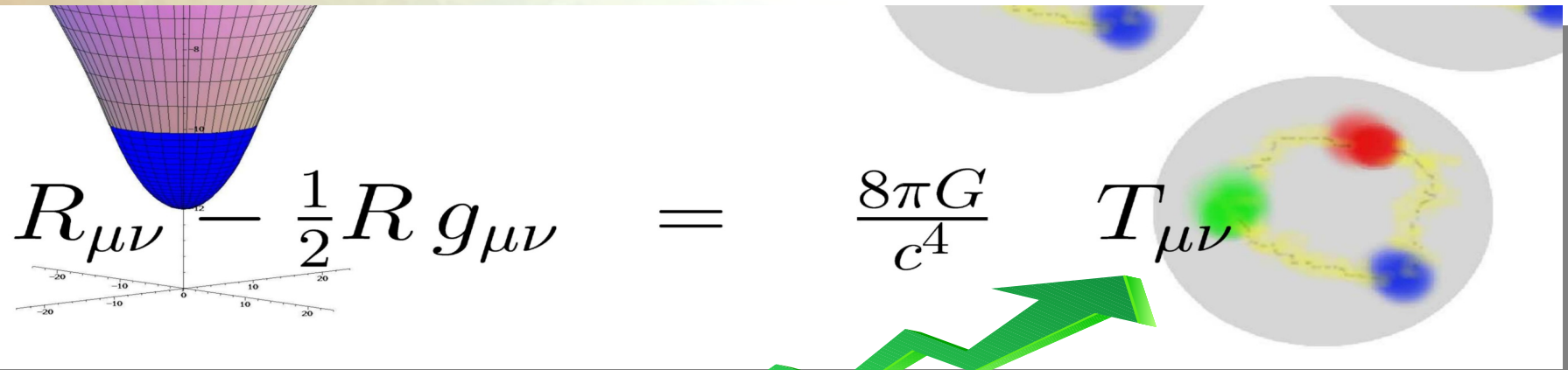erbrace{+\, G_S \sum_{j=0}^{8}\left[\left(\overline{\psi}\,\frac{\lambda_j}{2}\,\psi\right)^2 + \left(\overline{\psi}\,\frac{i\gamma_5\lambda_j}{2}\,\psi\right)^2\right]}_{\text{Skalare Wechselwirkung}}$$

$$\underbrace{-\, G_V \sum_{j=0}^{8}\left[\left(\overline{\psi}\,\gamma_\mu\frac{\lambda_j}{2}\,\psi\right)^2 + \left(\overline{\psi}\,\gamma_\mu\frac{\gamma_5\lambda_j}{2}\,\psi\right)^2\right]}_{\text{Vektorielle Wechselwirkung}} \qquad \psi \;\equiv\; \psi_{Aa}^{f}$$

$$\underbrace{-\, K\left[\det_f\left(\overline{\psi}\,(1-\gamma_5)\,\psi\right) + \det_f\left(\overline{\psi}\,(1+\gamma_5)\,\psi\right)\right]}_{\text{Flavour Mischterme}} + \underbrace{\mathcal{L}_L}_{\text{Leptonische Beiträge}}$$

MIT-Bag model

$$\epsilon^Q \;=\; \sum_{f=u,d,s} \frac{\nu_f}{2\pi^2} \int_0^{k_F^f} k^2 \sqrt{m_f^2 + k^2}\; dk \;+\; B$$

$$P^Q \;=\; \sum_{f=u,d,s} \frac{\nu_f}{6\pi^2} \int_0^{k_F^f} \frac{k^4}{\sqrt{m_f^2 + k^2}}\; dk \;-\; B\,,$$

The Gibbs Construction

Hadronic and quark surface:
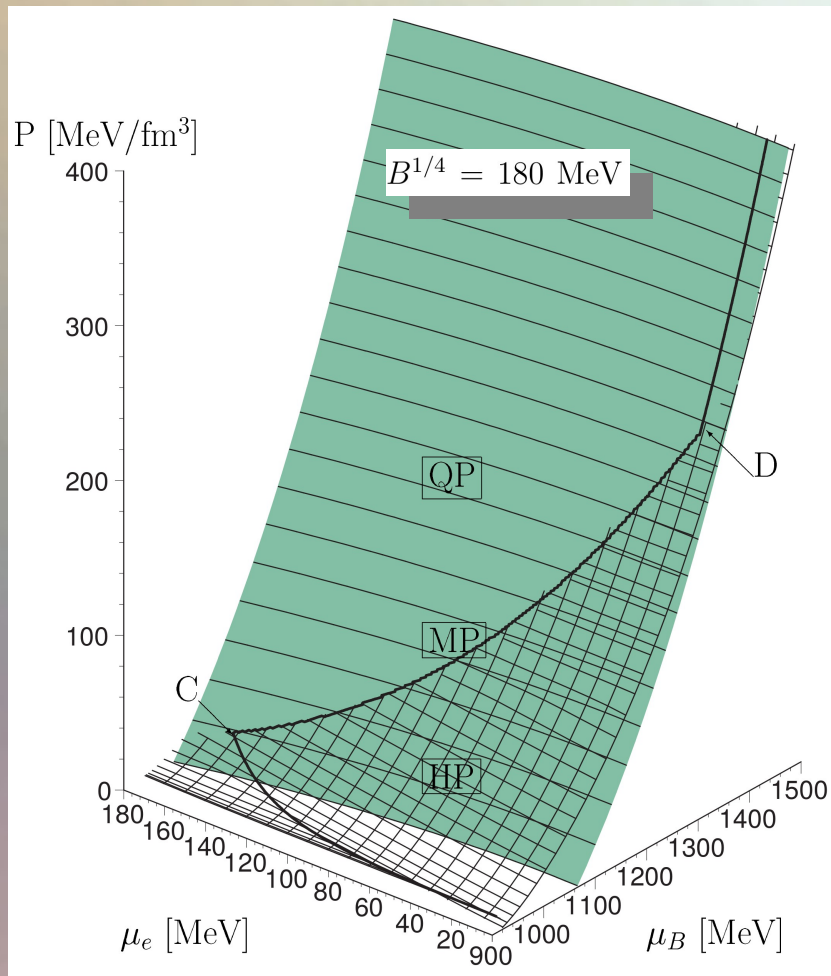
Charge neutrality condition is only globally realized

$$\rho_e := (1 - \chi)\rho_e^H(\mu_B, \mu_e) + \chi\rho_e^Q(\mu_B, \mu_e) = 0\,.$$

The pressure in the mixed phase depends on two independent chemical potentials
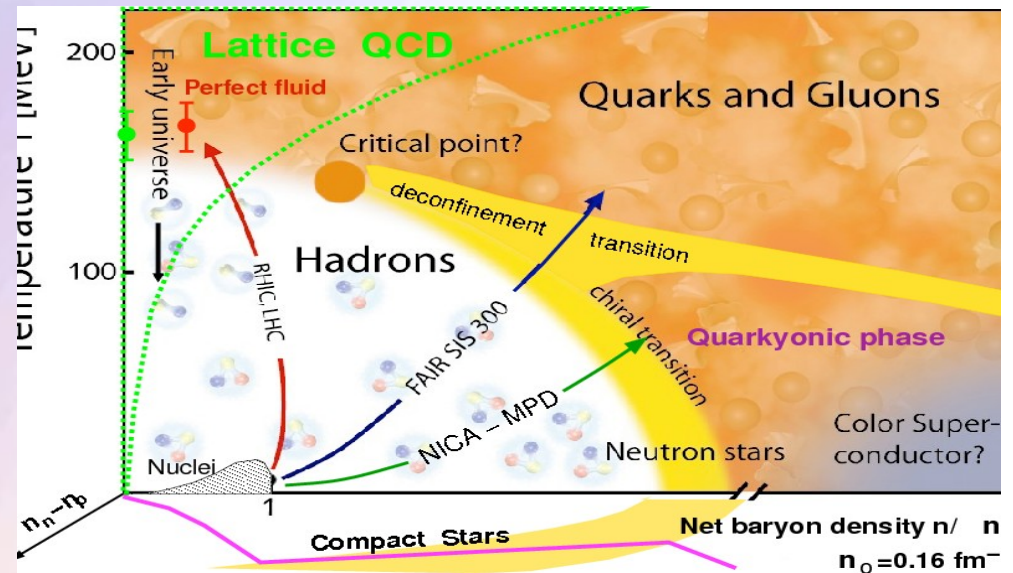
$$\begin{aligned} P^H(\mu_B, \mu_e) &= P^Q(\mu_B, \mu_e)\,, \\ \mu_B = \mu_B^H &= \mu_B^Q\,, \\ \mu_e = \mu_e^H &= \mu_e^Q \end{aligned}$$

The Gibbs Construction

Hadronic and quark surface:

Particle composition:

The Gibbs Construction

Hadronic and quark surface:

Particle composition:

M. Hanauske, Dissertation, "Properties of Compact Stars within QCD-motivated Models"
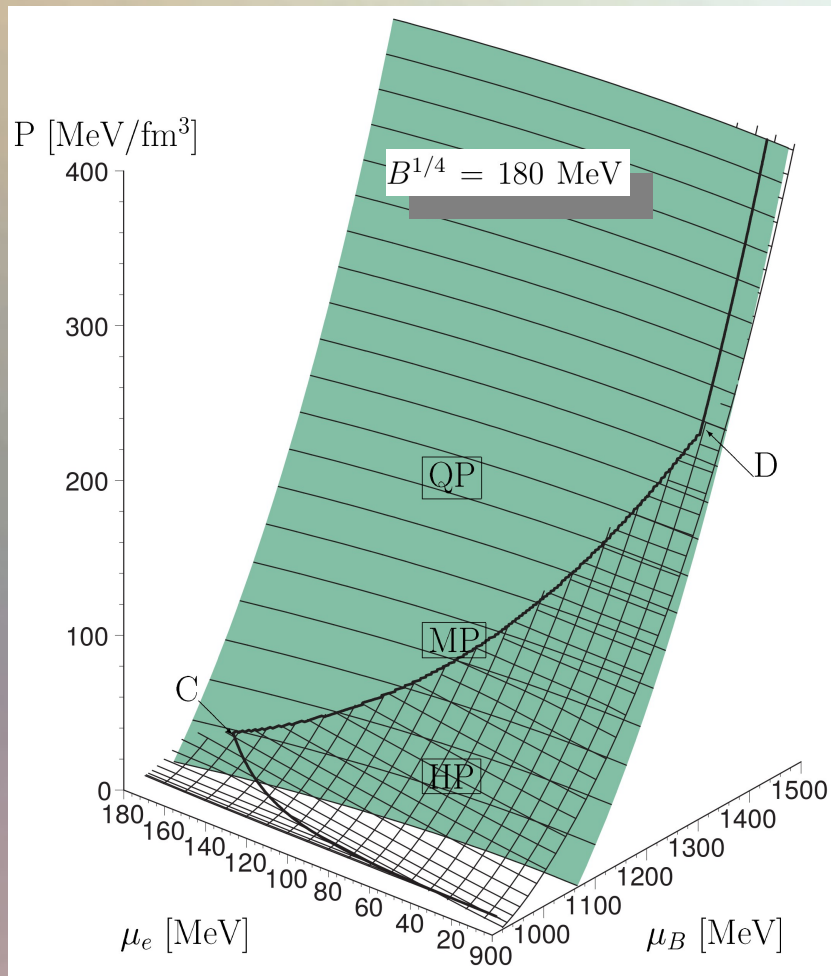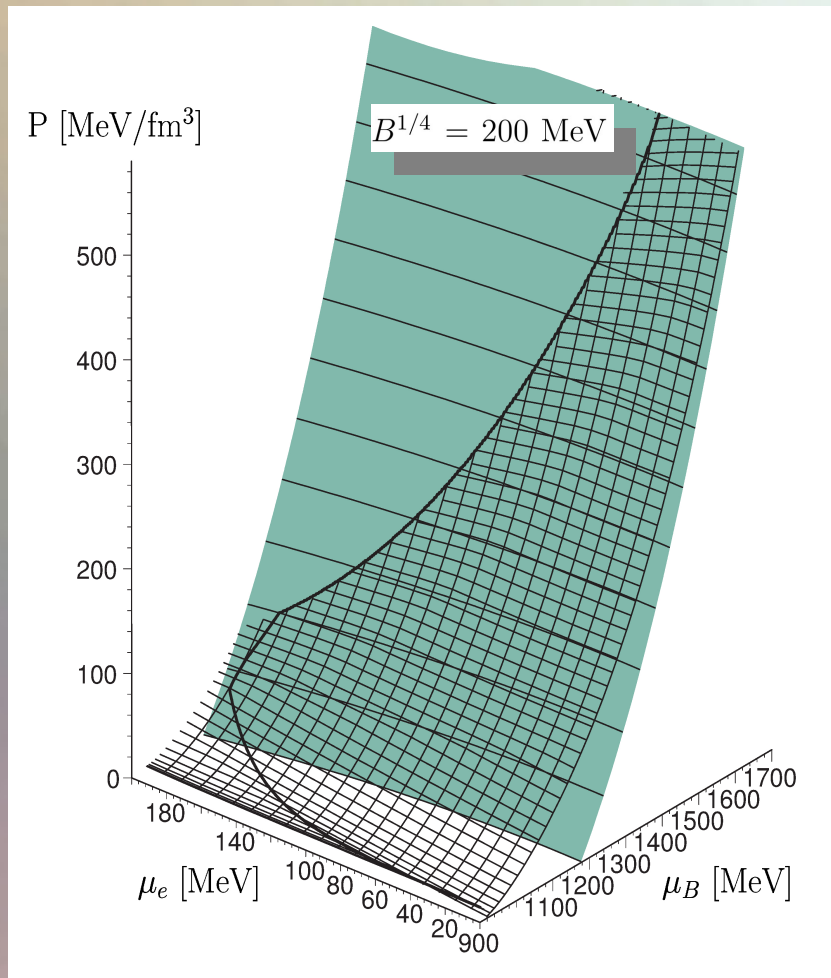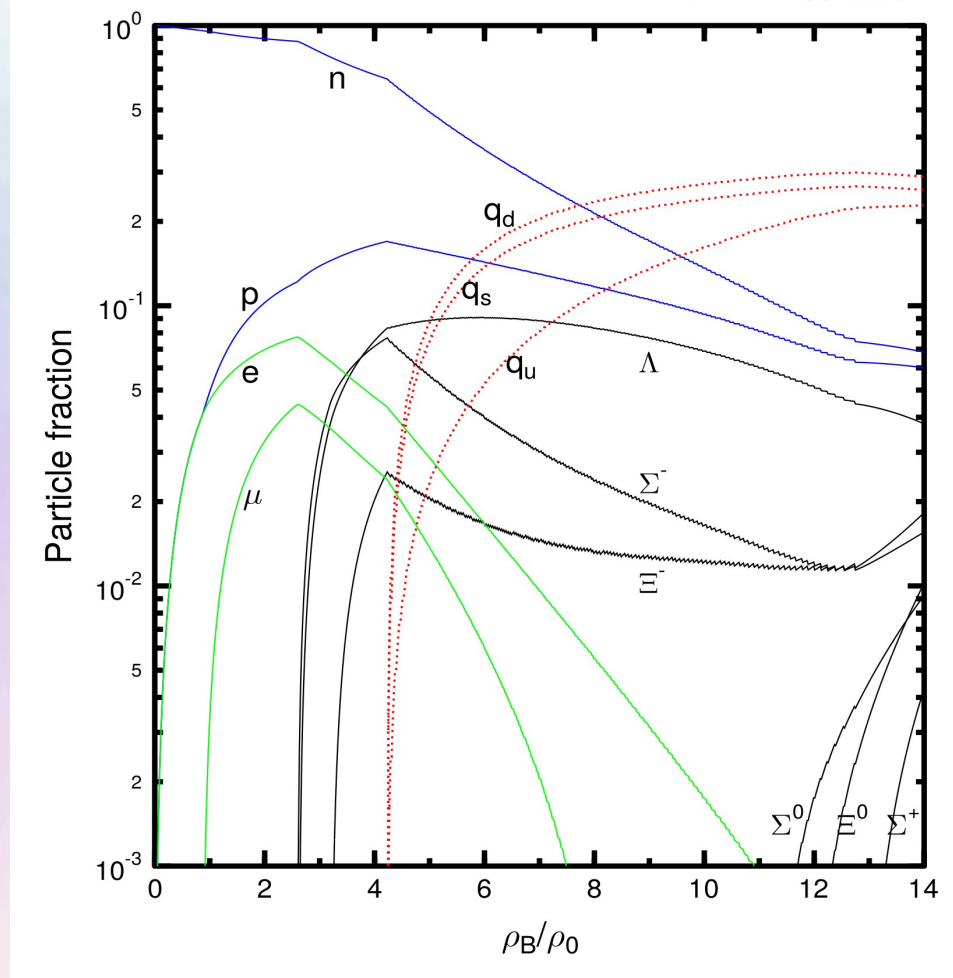
The Twin Star Collapse

Usually it is assumed that this loss of stability leads to the collapse into a black hole. However, realistic calculations open another possibility: th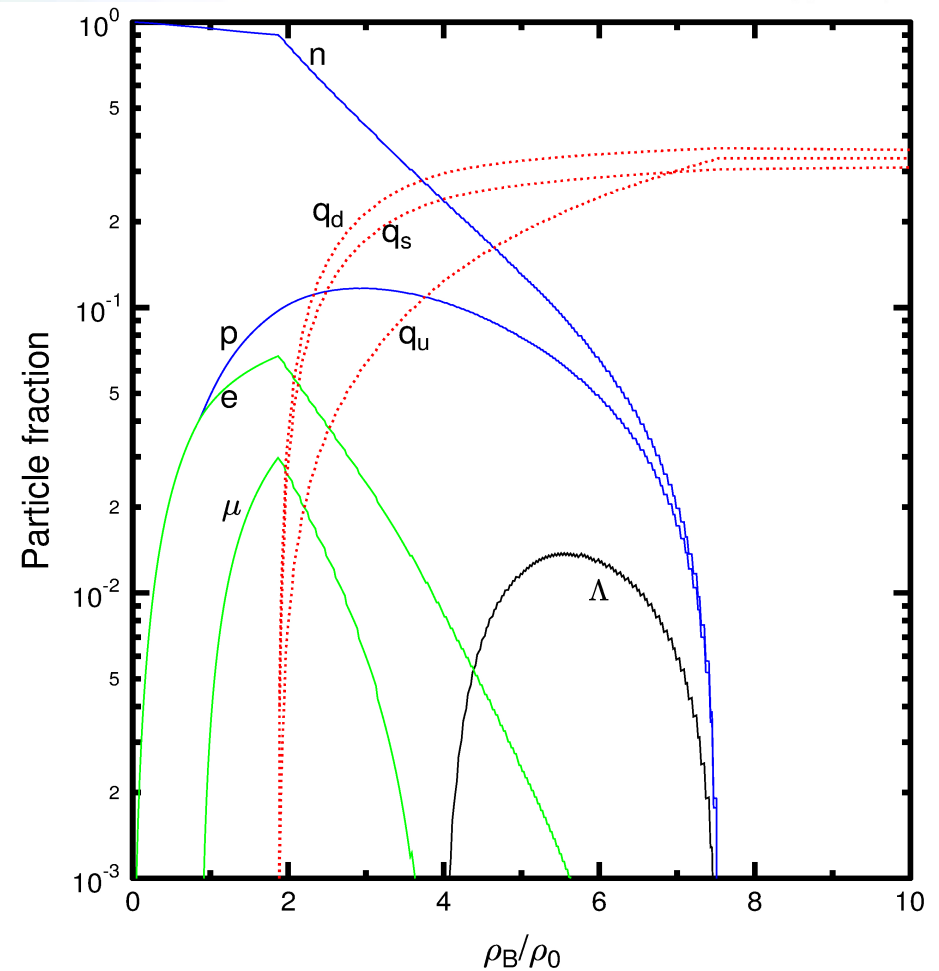e collapse into the twin star on the second sequence. A star from the first sequence which reaches the maximum mass (point A) will collapse to its twin star. The latter is the corresponding star on the second sequence, i.e. the one which has the same total baryon number (point B).

I.N. Mishustin, M. Hanauske, A. Bhattacharyya, L.M. Satarov, H. Stöcker, and W. Greiner, "Catastrophic rearrangement of a compact star due to quark core formation", Physics Letters B 552 (2003) p.1-8
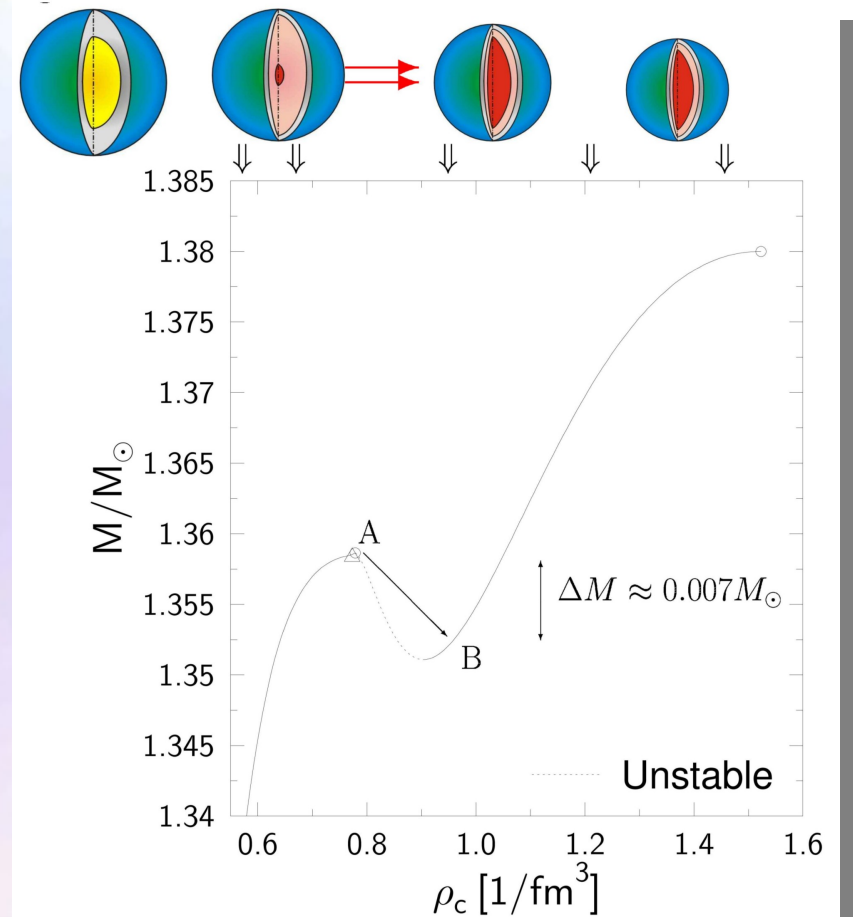
The Twin Star Collapse

Density profiles of the two twins
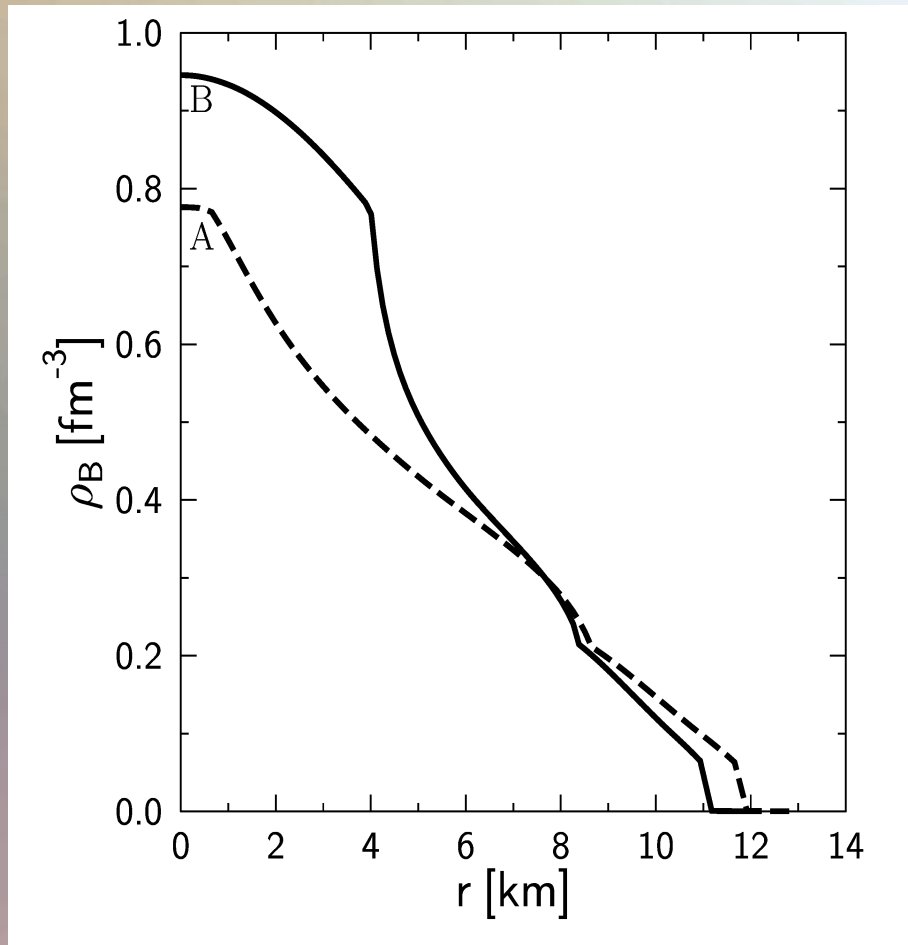
Conservation of total baryonic mass
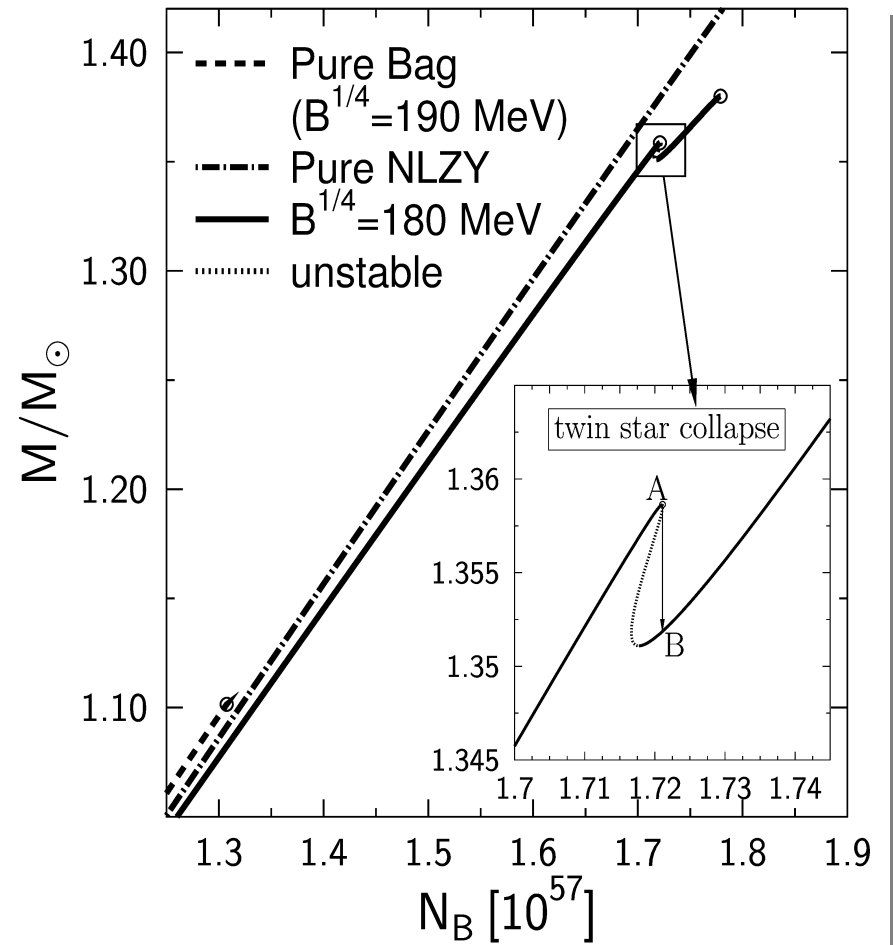
The Maxwell Construction

If the surface tension between the hadron and quark phase is relatively large, the mixed phase could completely disappear, so that a sharp boundary between the two phase appears. The Hadron-quark phase transition is then described using a Maxwell construction.

Pressure and baryon chemical potential stays constant, while the density and the charge chemical potential jump discontinuously during the phase transition.
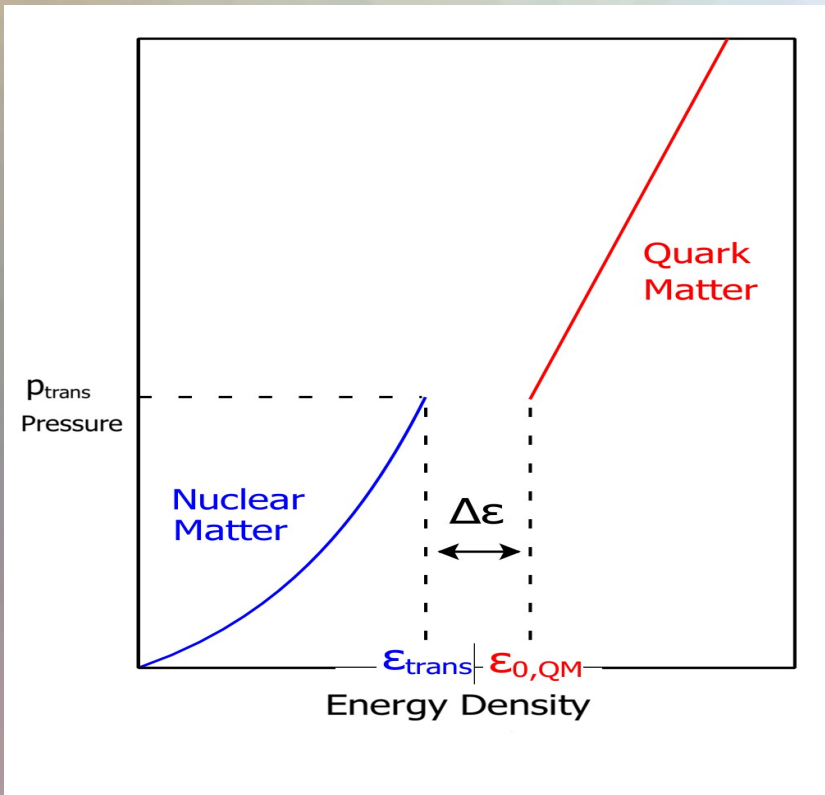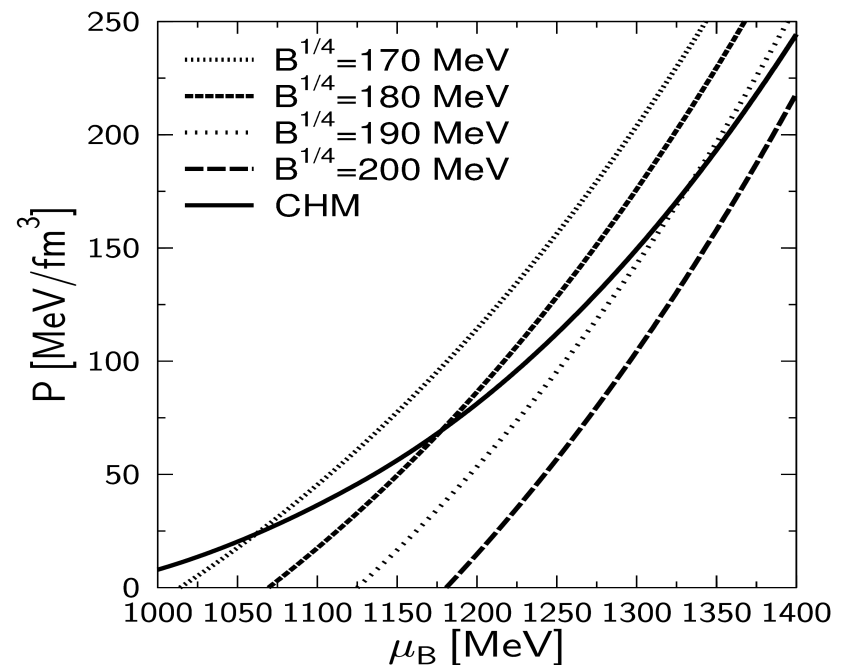
Image from M.G. Alford, S. Han, and M. Prakash, Phys. Rev. D 88, 083013 (2013)

Hybrid Star Properties

In contrast to the Gibbs construction, the star's density profile within the Maxwell construction (see right figure) will have a huge density jump at the phase transition boundary. Twin star properties can be found more easily when using a Maxwell construction.

Mass-Density relation
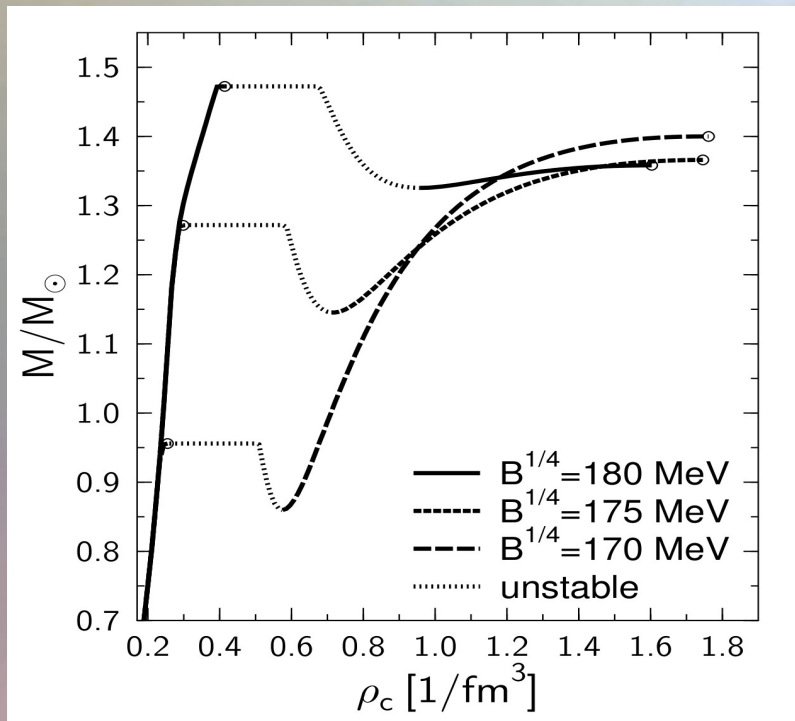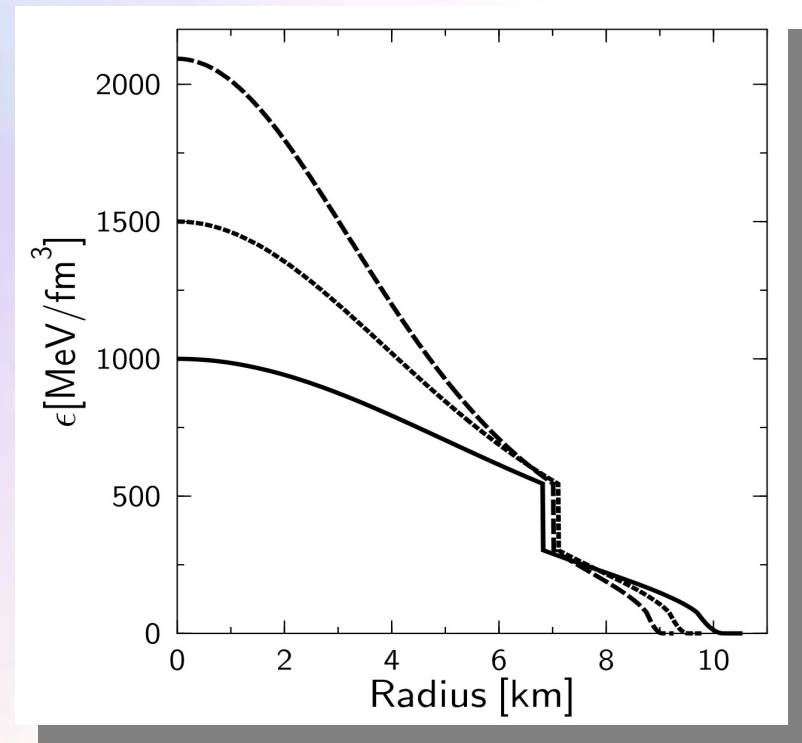
Energy-density profiles

Matthias Hanauske: "How to detect the QGP with telescopes", GSI Annual Report 2003, p.96

Numerical General Relativity in the context of the Hadron-Quark Phase Transition in Compact Stars

1. Introduction
2. The Hadron-Quark Phase Transition in the Interior of Compact Stars
3. Neutron Stars, Hybrid Stars and Quark Stars
4. **Numerical General Relativity and Relativistic Hydrodynamics**

Relativistic Hydrodynamics and Numerical General Relativity

A realistic numerical simulation of a twin star collapse, a merger of two compact stars or a collapse to a black hole, needs to go beyond a static, spherically symmetric TOV-solution of the Einstein- and Hydrodynamical equations.

$$R_{\mu\nu} - \frac{1}{2}g_{\mu\nu}R = 8\pi T_{\mu\nu}$$

$$\nabla_\mu(\rho u^\mu) = 0\,,$$
$$\nabla_\nu T^{\mu\nu} = 0\,.$$
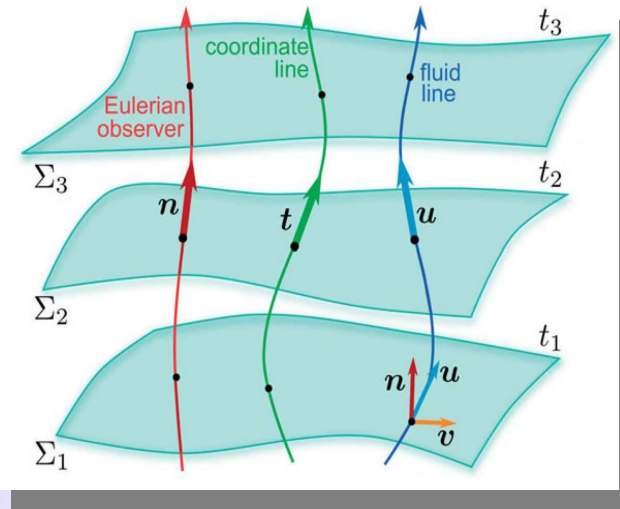
$$g_{\mu\nu} = \begin{pmatrix} -\alpha^2 + \beta_i\beta^i & \beta_i \\ \beta_i & \gamma_{ij} \end{pmatrix}$$

(3+1) decomposition of spacetime

$$d\tau^2 = \alpha^2(t, x^j)dt^2$$

$$x^i_{t+dt} = x^i_t - \beta^i(t, x^j)dt$$

The ADM equations

The ADM (Arnowitt, Deser, Misner) equations come from a reformulation of the Einstein equation using the (3+1) decomposition of spacetime.

$$\partial_t \gamma_{ij} = -2\alpha K_{ij} + \mathcal{L}_{\boldsymbol{\beta}}\gamma_{ij}$$
$$= -2\alpha K_{ij} + D_i\beta_j + D_j\beta_i$$

$$\partial_t K_{ij} = -D_i D_j \alpha + \beta^k \partial_k K_{ij} + K_{ik}\partial_j\beta^k + K_{kj}\partial_i\beta^k$$
$$+ \alpha\left({}^{(3)}R_{ij} + K K_{ij} - 2K_{ik}K^k_{\ j}\right) + 4\pi\alpha\left[\gamma_{ij}(S - E) - 2S_{ij}\right]$$

Time evolving part of ADM
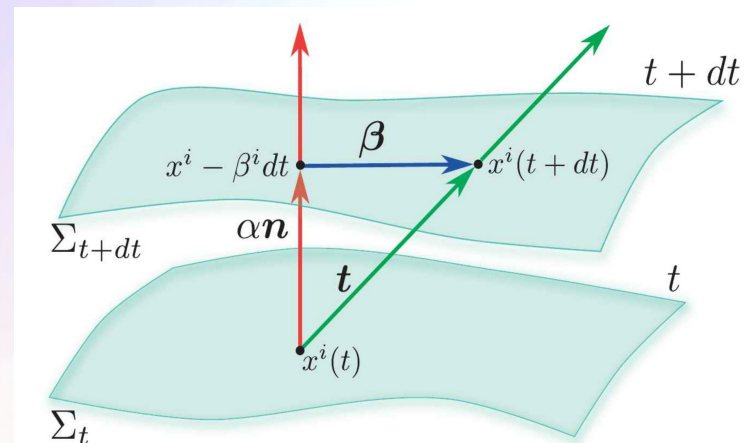
$$D_j(K^{ij} - \gamma^{ij}K) = 8\pi S^i$$

$${}^{(3)}R + K^2 - K_{ij}K^{ij} = 16\pi E$$

Constraints on each hypersurface

Three dimensional covariant derivative

$$D_\nu := \gamma^\mu_{\ \nu}\nabla_\mu = (\delta^\mu_\nu + n_\nu n^\mu)\nabla_\mu$$

Three dimensional Riemann tensor

$${}^{(3)}R^\mu_{\ \nu\kappa\sigma} = \partial_\kappa {}^{(3)}\Gamma^\mu_{\nu\sigma} - \partial_\sigma {}^{(3)}\Gamma^\mu_{\nu\kappa} + {}^{(3)}\Gamma^\mu_{\lambda\kappa}{}^{(3)}\Gamma^\lambda_{\nu\sigma} - {}^{(3)}\Gamma^\mu_{\lambda\sigma}{}^{(3)}\Gamma^\lambda_{\nu\kappa}$$

$${}^{(3)}\Gamma^\alpha_{\beta\gamma} = \frac{1}{2}\gamma^{\alpha\delta}\left(\partial_\beta\gamma_{\gamma\delta} + \partial_\gamma\gamma_{\delta\beta} - \partial_\delta\gamma_{\beta\gamma}\right)$$

Spatial and normal projections of the energy-momentum tensor:

$$S_{\mu\nu} := \gamma^\alpha_{\ \mu}\gamma^\beta_{\ \nu}T_{\alpha\beta},$$
$$S_\mu := -\gamma^\alpha_{\ \mu}n^\beta T_{\alpha\beta},$$
$$S := S^\mu_{\ \mu},$$
$$E := n^\alpha n^\beta T_{\alpha\beta},$$

Extrinsic Curvature:

$$K_{\mu\nu} := -\gamma^\lambda_{\ \mu}\nabla_\lambda n_\nu$$
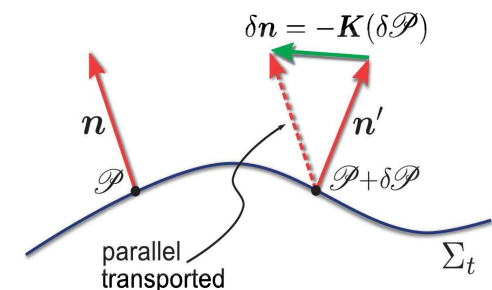
From ADM to BSSNOK

Unfortunately the ADM equations are only weakly hyperbolic (mixed derivatives in the three dimensional Ricci tensor) and therefore not "well posed". It can be shown that by using a conformal traceless transformation, the ADM equations can be written in a hyperbolic form. This reformulation of the ADM equations is known as the BSSNOK (Baumgarte, Shapiro, Shibata, Nakamuro, Oohara, Kojima) formulation of the Einstein equation. Most of the numerical codes use this (or the CCZ4) formulation.

The 3+1 Valencia Formulation of the Relativistic Hydrodynamic Equations

$$\nabla_\mu(\rho u^\mu) = 0 \,,$$
$$\nabla_\nu T^{\mu\nu} = 0 \,.$$

To guarantee that the numerical solution of the hydrodynamical equations (the conservation of rest mass and energy-momentum) converge to the right solution, they need to be reformulated into a conservative formulation. Most of the numerical "hydro codes" use here the 3+1 Valencia formulation.

Finite difference methods

Discretisation of a hyperbolic initial value boundary problem.
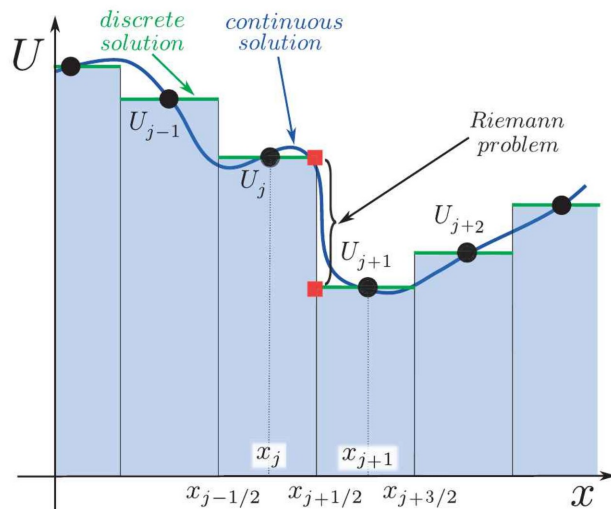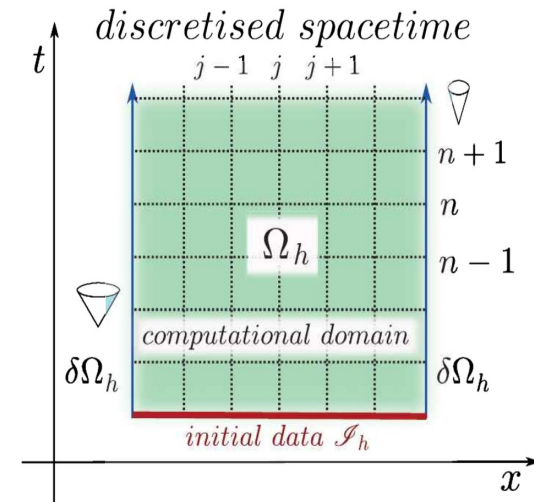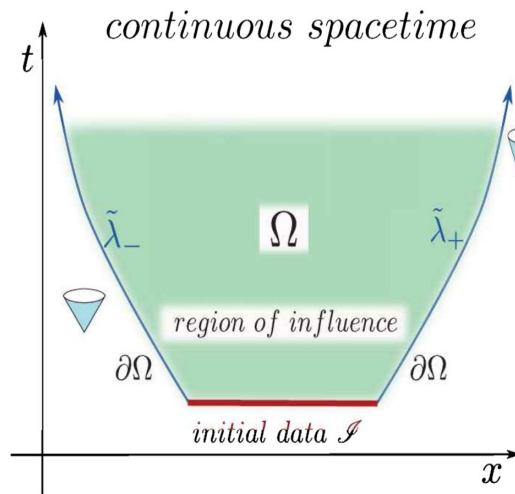
High resolution shock capturing methods (HRSC methods) are needed, when Riemann problems of discontinuous properties and shocks needs to be evolved accurately

All figures from: Luciano Rezzolla, Olindo Zanotti: Relativistic Hydrodynamics, Oxford Univ. Press, Oxford (2013)

Mergers of two Hybrid Stars

The frequency spectrum of the emitted gravitational wave reflects some of the properties of the equation of state (K.Takami, L.Rezzolla, and L.Baiott, "Constraining the Equation of State of Neutron Stars from Binary Mergers", arXiv:1403.5672). Whether a Hadron-Quark phase transition is present during merger should be visible using gravitational wave detectors. The following results represent a hybrid star merger calculation (EOS: ALF2 (APR-Hadronic model +Gibbs construction of MIT-Bag+CFL-Phase), see Alford et.al.,APJ 629,2005) where the EOS was fitted with a piecewise polytrope.
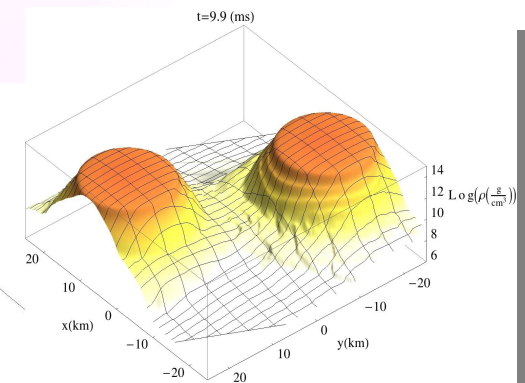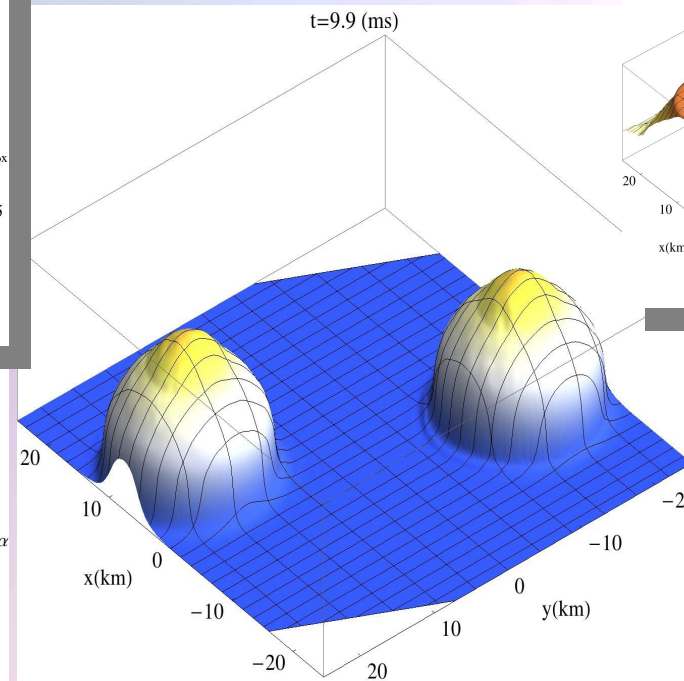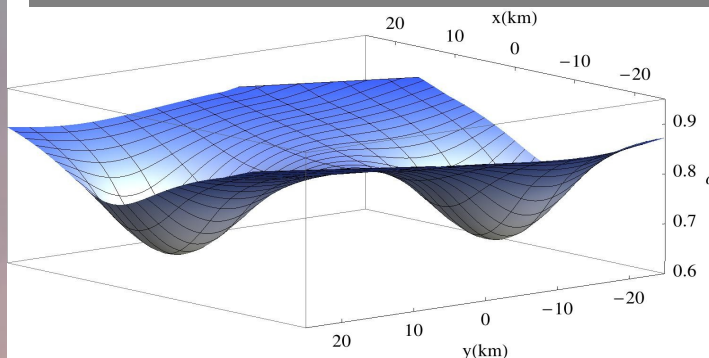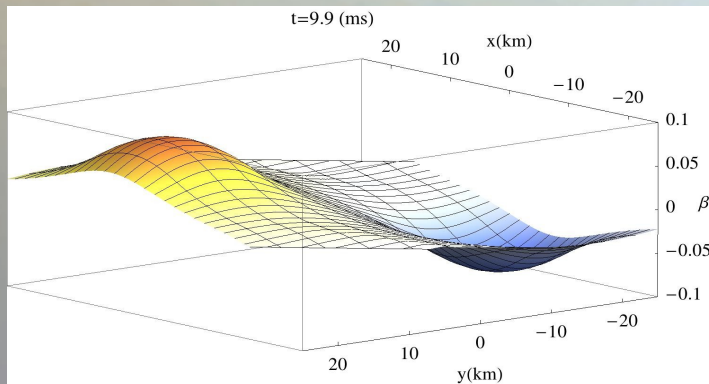
Simulations done by Kentaro Takami

Collapse Scenario of a Hybrid Star

The gravitational collapse of a hybrid star to a black hole is visualized on the right side within a space-time diagram of the Schwarzschild metric in advanced Eddington-Finkelstein coordinates.

The formation of the apparent and event horizon of the black hole confines the quark star macroscopically. Finally the colour charge of the deconfined free quarks cannot be observed from outside.
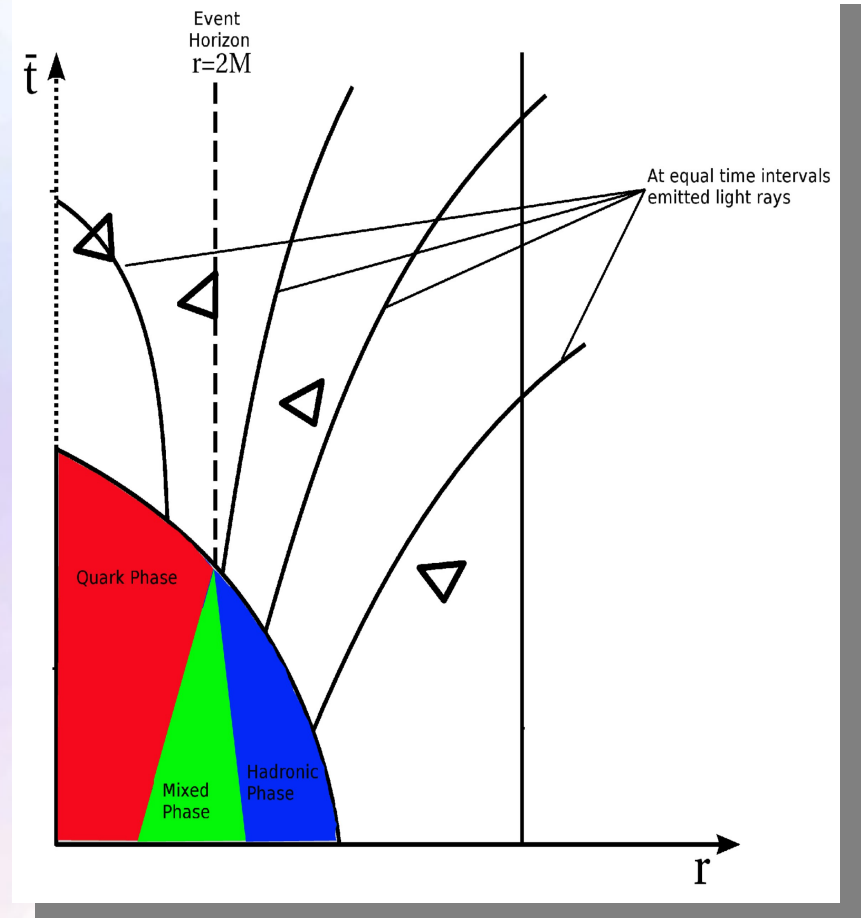
End

- ....

Observed Masses of Compact Star Binaries

PSR J1906+0746 Van Leeuwen et al, arXiv:1411.1518

144-ms pulsar, discovered in in 2004
Orbital period: 3.98 hours, Eccentricity: 0.085
Pulsar mass: 1.291(11), Companion mass 1.322(11)
Observed between 1998-2009,
then it disappeared due to spin precession

Double Pulsar PSR J0737-3039

Orbital period: 147 min, Eccentricity: 0.088
pulsar A: P=23 ms, M=1.3381(7)
pulsar B: P=2.7 s, M=1.2489(7)
Pulsar A is eclipsed once per orbit by B (for 30 s)
 Kramer, Wex, Class. Quantum Grav. 2009

PSR J0348+0432

Orbital Period:
2.46 hours

Pulsar mass:
2.01+-0.04

white dwarf mass:
0.172+-0.003

Picture from J. Antoniadis et.al. Science 2013

updated 15 January 2014

X-ray/Optical binaries

4U1700-37 (a)
Vela X-1 (b)
Cyg X-2 (d)
4U1538-52 (b)
SMC X-1 (T)
LMC X-4 (b)
Cen X-3 (b)
Her X-1 (b)
XTE J2123-058 (l)
2S 0921-630 (F)
4U1822-371 (n)
EXO1722-363 (I)
B1957+20 (Q) black widow pulsar
IFE J18027-2016 (c)
OAO 1657-415 (w)
J1311-3430 (R)
J01326.7+303228 (L) bwp

double neutron star binaries

J1829+2456 (z)
J1829+2456 comp.
J1811-1736 (A)
J1811-1736 comp.
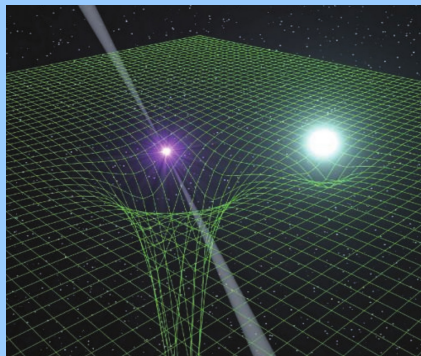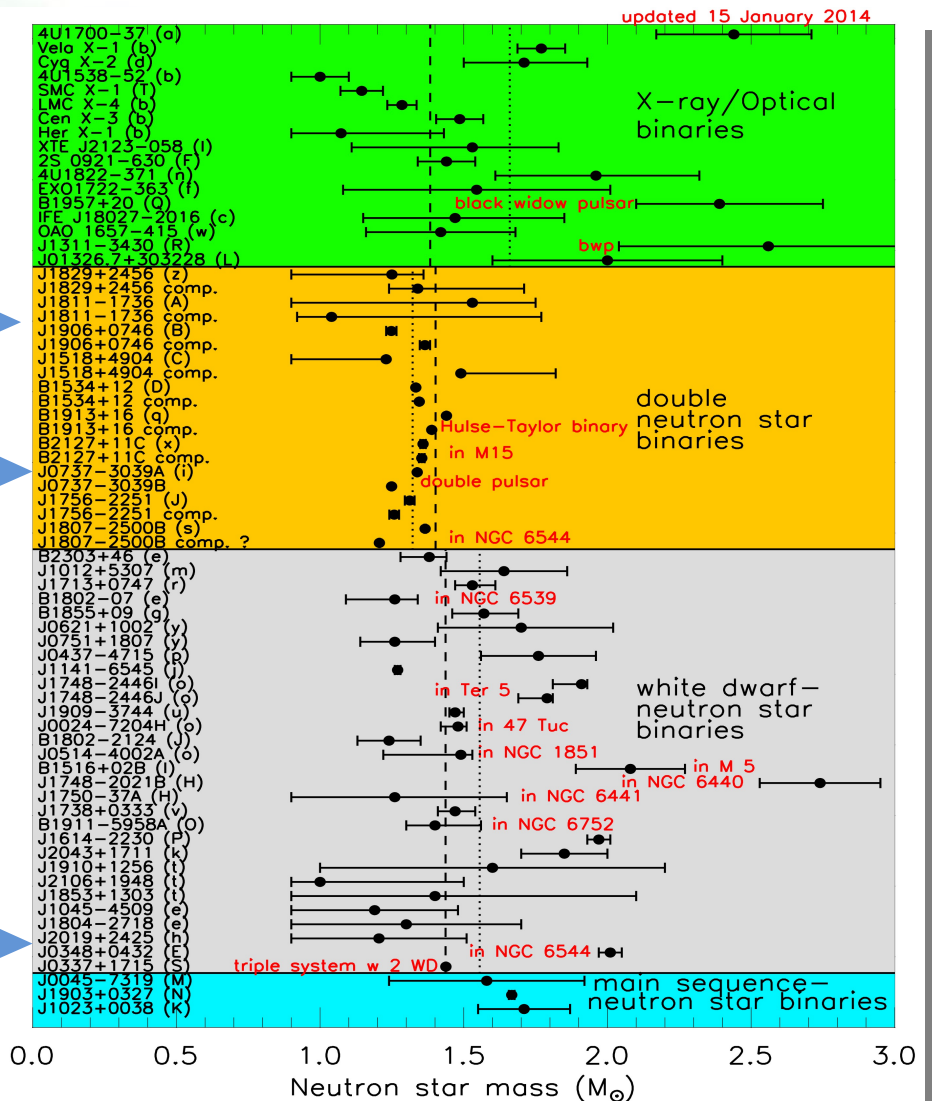J1906+0746 (B)
J1906+0746 comp.
J1518+4904 (C)
J1518+4904 comp.
B1534+12 (D)
B1534+12 comp.
B1913+16 (q) Hulse-Taylor binary
B1913+16 comp.
B2127+11C (x) in M15
B2127+11C comp.
J0737-3039A (i) double pulsar
J0737-3039B
J1756-2251 (J)
J1756-2251 comp.
J1807-2500B (s) in NGC 6544
J1807-2500B comp. ?

white dwarf– neutron star binaries

B2303+46 (e)
J1012+5307 (m)
J1713+0747 (r)
B1802-07 (e) in NGC 6539
B1855+09 (g)
J0621+1002 (y)
J0751+1807 (y)
J0437-4715 (p)
J1141-6545 (j)
J1748-2446I (o) in Ter 5
J1748-2446J (o)
J1909-3744 (u)
J0024-7204H (o) in 47 Tuc
B1802-2124 (J)
J0514-4002A (o) in NGC 1851
B1516+02B (H) in M 5
J1748-2021B (H) in NGC 6440
J1750-37A (H) in NGC 6441
J1738+0333 (v)
B1911-5958A (O) in NGC 6752
J1614-2230 (P)
J2043+1711 (k)
J1910+1256 (t)
J2106+1948 (t)
J1853+1303 (t)
J1045-4509 (e)
J1804-2718 (e)
J2019+2425 (h)
J0348+0432 (E) in NGC 6544
J0337+1715 (S) triple system w 2 WD

main sequence– neutron star binaries

J0045-7319 (M)
J1903+0327 (N)
J1023+0038 (K)

0.0   0.5   1.0   1.5   2.0   2.5   3.0
Neutron star mass (M$_\odot$)

Summary: Neutron Stars

Schematic Structure of a Neutron Star

Outer Envelopes

The outer envelopes of a neutron star constist of a thin plasma atmosphere where the thermal radiation is formed and a outer and inner crust which consist of electrons and nuclei. The whole outer envelope is about one kilometer thick and it occupies the density range $\epsilon \leq 0.5\,\epsilon_0$.
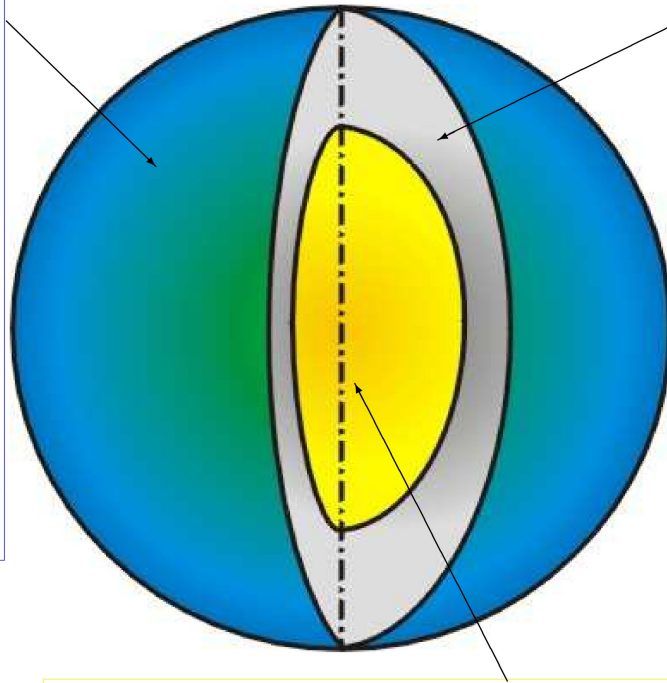
Outer Core

The outer core consists mainly of neutrons with several per cent admixture of protons, electrons and myons. It is several kilometers thick and occupies the density range $0.5\,\epsilon_0 < \epsilon \leq 2\,\epsilon_0$.

Nuclear matter density:
$\epsilon_0 = 2.8 \cdot 10^{14} \text{ g/cm}^3$

Inner Core

In the inner core of a neutron star hyperonic particles ($\Sigma^-, \Lambda, \Xi...$) are present. The inner core extends to the center of the star where its central density can be as high as $\epsilon \approx 15\,\epsilon_0$.

Neutron Star Matter
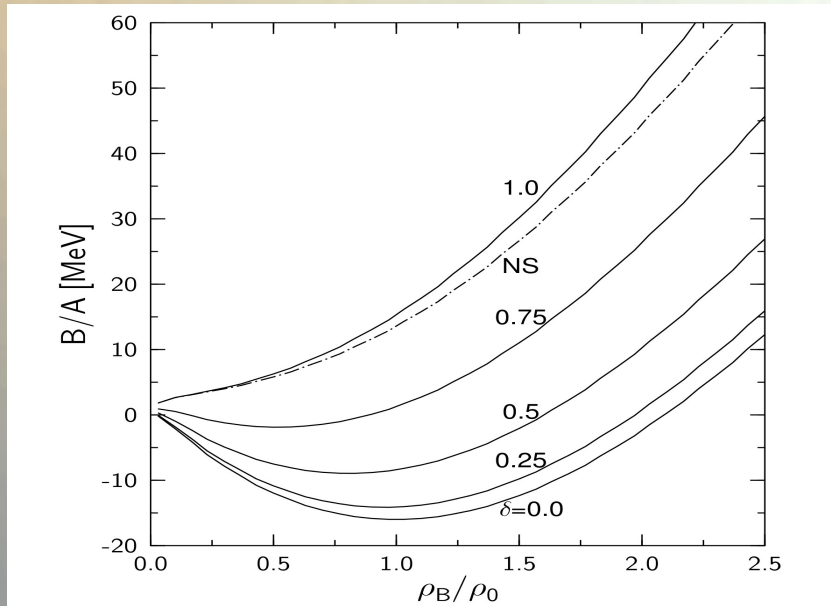
Binding energy per nucleon as a function of the baryonic density for different values of the neutron-proton asymmetry δ. 'NS' describes charge-neutral neutron star matter in β-equilibrium.

1) The equation of state (pressure P of the hadronic matter vs. the baryonic density). The solid curve (npe) describes charge-neutral matter in β-equilibrium consisting of neutrons, protons and electrons, whereas the dotted curve (npeμY) includes muons and hyperons.

In contrast to normal nuclear matter, neutron star matter needs to fulfil three additional conditions:

1) Charge Neutrality

2) β-equilibrium $\quad n \Leftrightarrow p + e + \tilde{\nu}_e$

3) Strangeness production

$$N + N \Rightarrow N + H + M \ ,$$
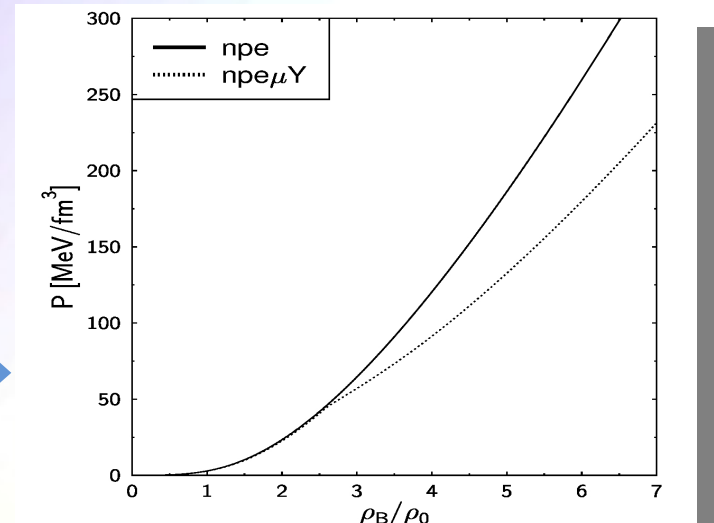
Hybrid Stars

To describe the properties of the Hadron-Quark phase transition happening in Hybrid stars an effective model for the quark phase is needed:

$$\lambda_j \equiv \lambda_{ja}{}^b$$

$$\mathcal{L} = \underbrace{\overline{\psi}\,(i\,\partial\!\!\!/ - \hat{m}_0)\,\psi}_{\text{Kinetische und Massenbeiträge}} + G_S \underbrace{\sum_{j=0}^{8}\left[\left(\overline{\psi}\,\frac{\lambda_j}{2}\,\psi\right)^2 + \left(\overline{\psi}\,\frac{i\gamma_5\lambda_j}{2}\,\psi\right)^2\right]}_{\text{Skalare Wechselwirkung}}$$

$$-G_V \underbrace{\sum_{j=0}^{8}\left[\left(\overline{\psi}\,\gamma_\mu\frac{\lambda_j}{2}\,\psi\right)^2 + \left(\overline{\psi}\,\gamma_\mu\frac{\gamma_5\lambda_j}{2}\,\psi\right)^2\right]}_{\text{Vektorielle Wechselwirkung}}$$

$$\psi \equiv \psi_{Aa}^f$$

$$\partial\!\!\!/ \equiv \partial\!\!\!/_A{}^B := \partial_\mu \gamma^\mu{}_A{}^B$$

$$-\underbrace{K\left[\det_f\left(\overline{\psi}\,(1-\gamma_5)\,\psi\right) + \det_f\left(\overline{\psi}\,(1+\gamma_5)\,\psi\right)\right]}_{\text{Flavour Mischterme}} + \underbrace{\mathcal{L}_L}_{\text{Leptonische Beiträge}}$$

Eg. the Nambu-Jona-Lasinio (NJL) Model or the
MIT-Bag model

$$\epsilon^Q = \sum_{f=u,d,s}\frac{\nu_f}{2\pi^2}\int_0^{k_F^f} k^2\sqrt{m_f^2 + k^2}\,dk \; + B$$

$$P^Q = \sum_{f=u,d,s}\frac{\nu_f}{6\pi^2}\int_0^{k_F^f} \frac{k^4}{\sqrt{m_f^2 + k^2}}\,dk \; - B\,,$$

A hybrid model of a compact star is realized by a construction of a phase transition between a hadronic model and a quark model. In contrast to the Maxwell construction of a phase transition, in a Gibbs construction a mixed phase is present in the stars interior, where both phases co-exist. In the mixed phase transition region each phase has a charge; only the overall electrical charge density vanishes. In the mixed phase, the pressure of the hadronic matter has to be equal to the pressure of the quark phase, whereas the particle and energy densities differ.

M. Hanauske, L.M. Satarov, I.N. Mishustin, H. Stöcker, and W. Greiner, Phys. Rev. D 64, 043005 (2001)

The Gibbs Construction

Since the charge neutrality condition is only globally realized, the pressure depends on two independently chemical potentials, the baryonic and charge chemical potential:

$$\begin{aligned} P^H(\mu_B, \mu_e) &= P^Q(\mu_B, \mu_e), \\ \mu_B = \mu_B^H &= \mu_B^Q, \\ \mu_e = \mu_e^H &= \mu_e^Q \end{aligned}$$

Charge density neutrality condition:

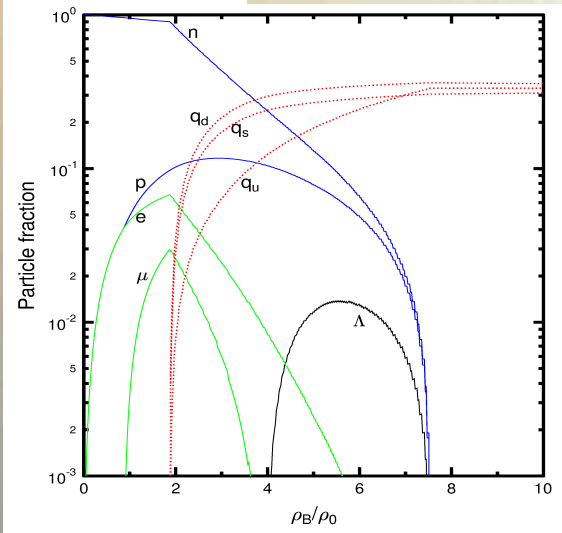$$\rho_e := (1 - \chi)\rho_e^H(\mu_B, \mu_e) + \chi\rho_e^Q(\mu_B, \mu_e) = 0.$$

Overall baryonic density:

$$\rho_B = (1 - \chi)\rho_B^H(\mu_B, \mu_e) + \chi\rho_B^Q(\mu_B, \mu_e),$$

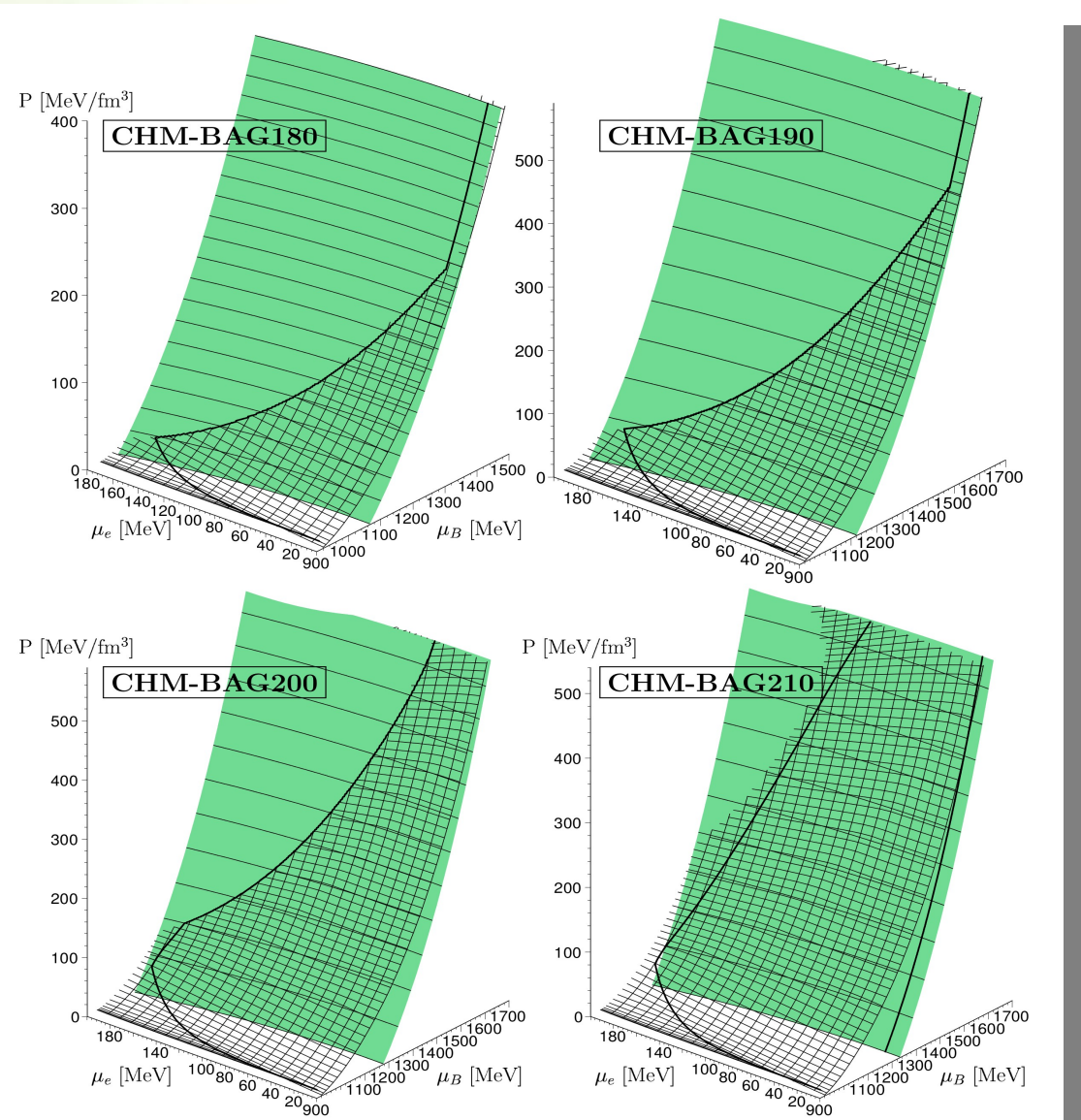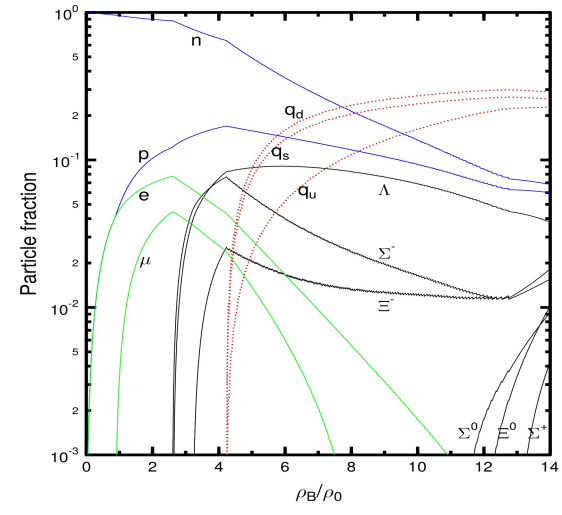$$\mu_i = B_i\,\mu_B + Q_i\,\mu_e$$

$$\begin{aligned} \mu_u &= \frac{1}{3}(\mu_B - 2\,\mu_e) \\ \mu_d = \mu_s &= \frac{1}{3}(\mu_B + \mu_e) \quad . \end{aligned}$$
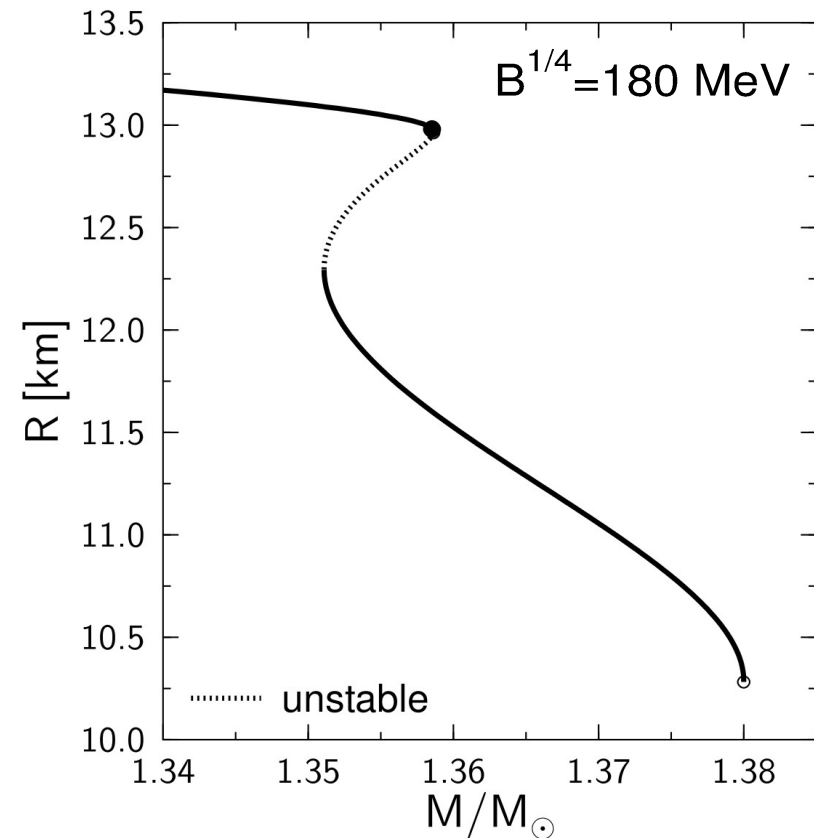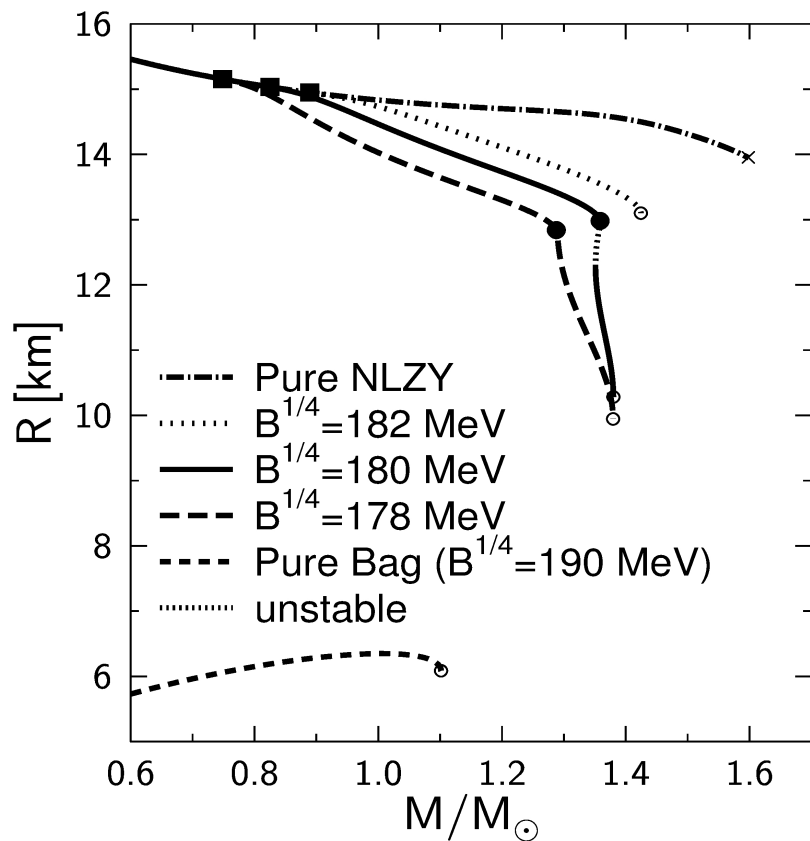
The Gibbs Construction

$B^{1/4} = 180$ MeV

$B^{1/4} = 200$ MeV

CHM-BAG180

CHM-BAG190

CHM-BAG200

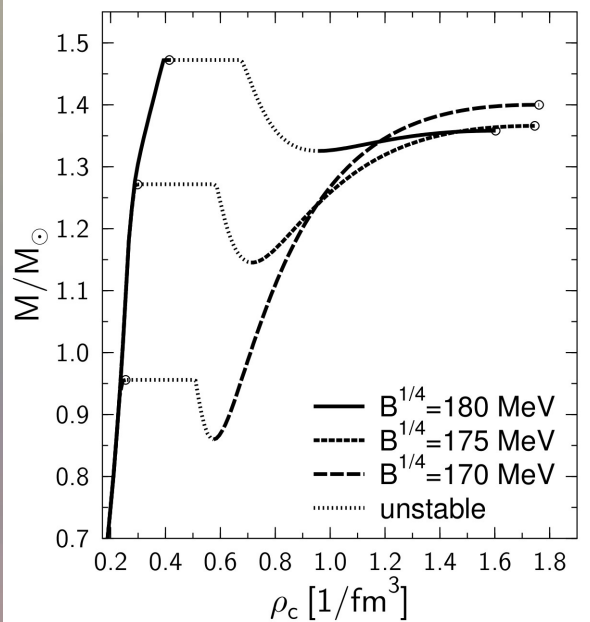CHM-BAG210

Hybrid Star Properties

Mass-Radius relations within a hybrid star model. The MIT-Bag model, for different values of the Bag parameter, was used for the quark phase, whereas for the hadronic phase the NLZY-model was used.

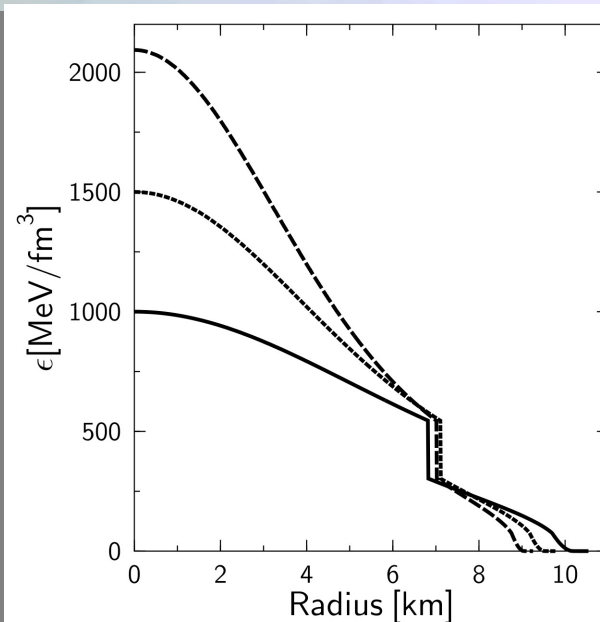M. Hanauske, Dissertation, "Properties of Compact Stars within QCD-motivated Models"

Hybrid Star Properties

In contrast to the Gibbs construction, the star's density profile within the Maxwell construction (see middle figure) will have a huge density jump at the phase transition boundary. Twin star properties can be found more easily when using a Maxwell construction (see left and right figure).
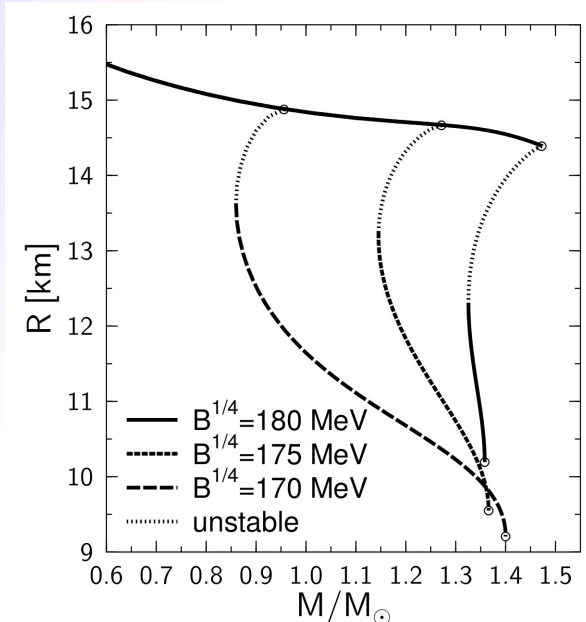
### Mass-Density relation

Energy-density profiles

Radius-Mass relation

Matthias Hanauske: "How to detect the QGP with telescopes", GSI Annual Report 2003, p.96

Exotic Stars

But, unfortunately, twin stars can not be created solely by a Hadron-Quark phase transition. Extremely bound hyperon mater, or kaon condensation could also form a twin star behaviour.

J. Schaffner-Bielich, M. Hanauske, H. Stöcker, and W. Greiner, Phys. Rev. Lett. 89, 171101 (2002)
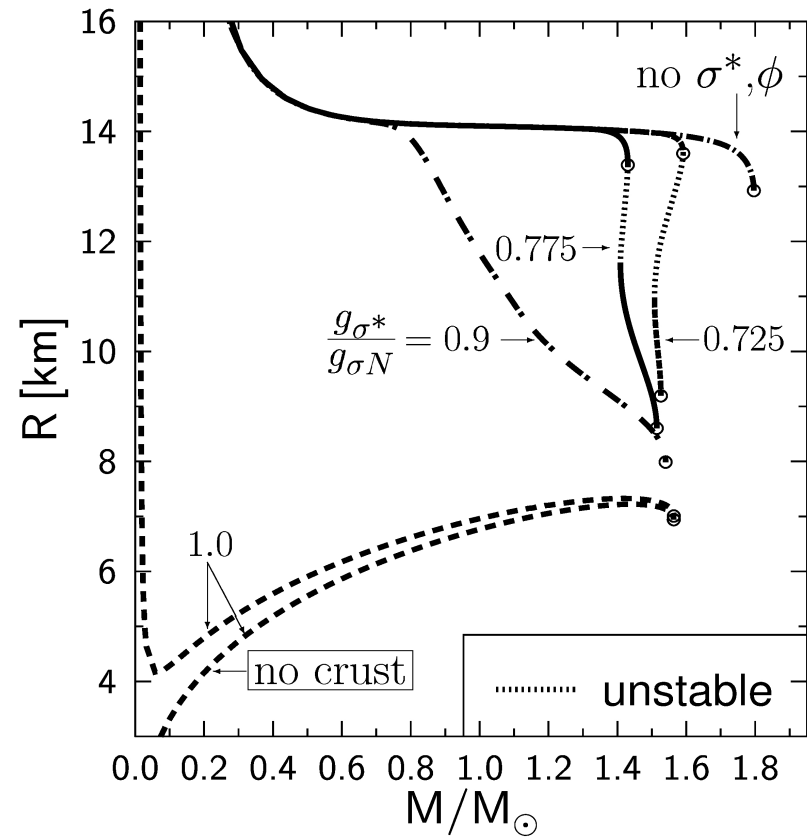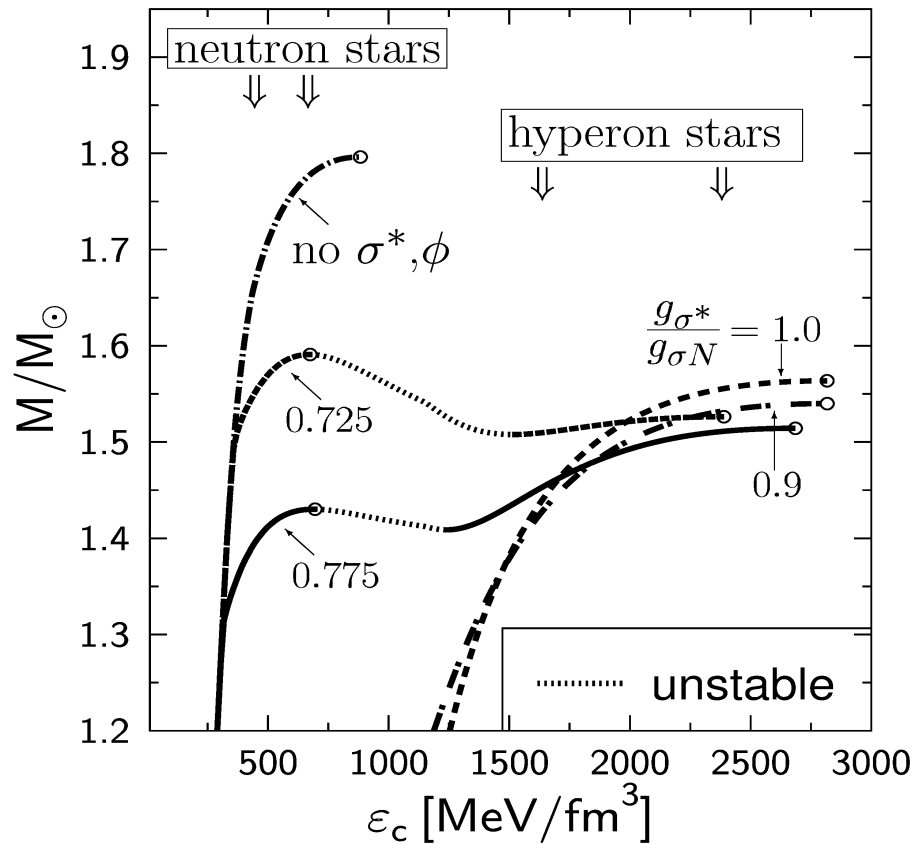
The Spin Up Effect

A rotating neutron star slowly loses its energy and angular momentum through electromagnetic and gravitational radiation with time. However, it conserves the total baryon number during this evolution. The Figures below show results of uniformly rotating compact stars including a Bose-Einstein condensates of antikaons. The Figure on the right shows the behavior of angular velocity with angular momentum. The mass shedding limit sequence is shown by a light solid line. The stable parts of the normal and supramassive sequences are displayed by dark solid lines and the unstable parts by dotted lines. Curve II indicates a collapse of a neutron star to an exotic star belonging to the third family of compact stars.

S. Banik, M. Hanauske, D. Bandyopadhyay, and W. Greiner, Phys. Rev. D 70, 123004 (2004)
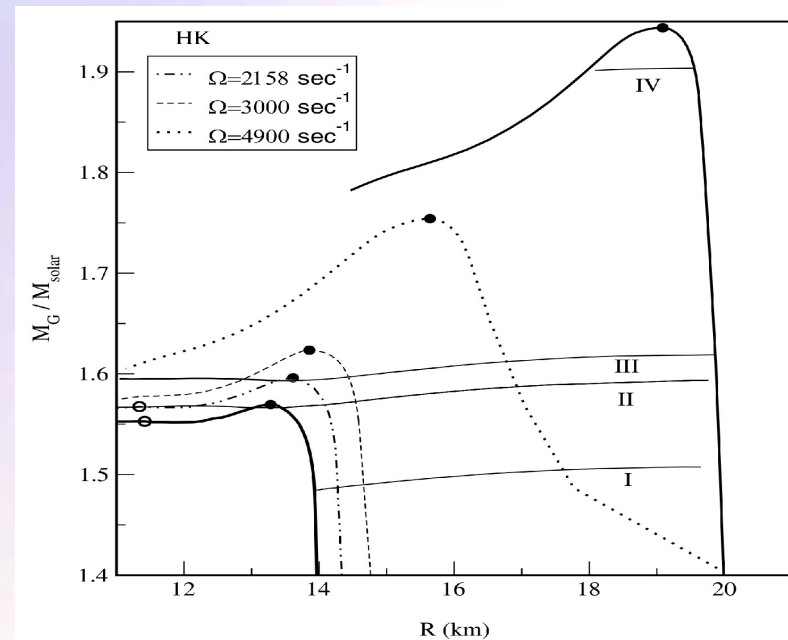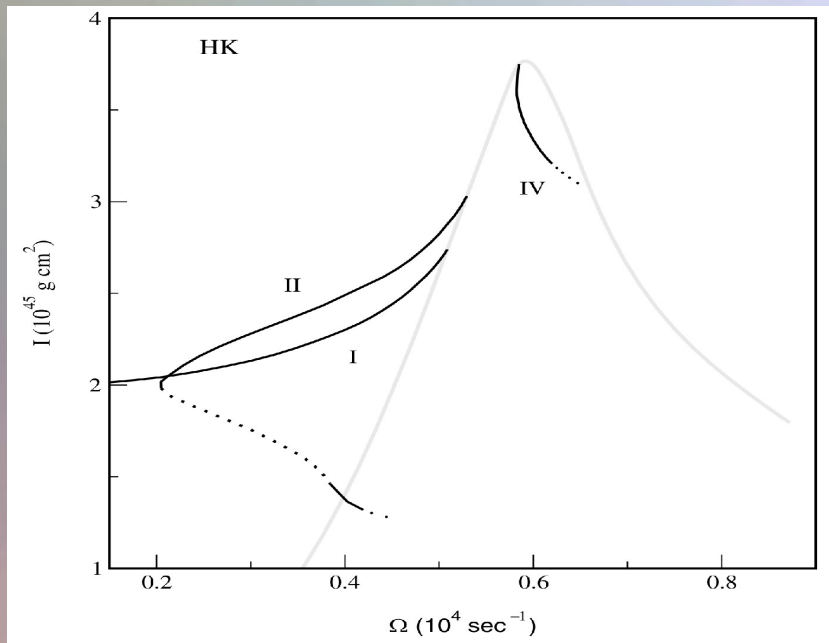
Gauge Conditions

On each spatial hypersurface, four additional degrees of freedom need to be specified: A *slicing condition* for the lapse function and a *spatial shift condition* for the shift vector need to be formulated to close the system. In an optimal gauge condition, singularities should be avoided and numerical calculations should be less time consuming.

Bona-Massó family of slicing conditions:

$$\partial_t \alpha - \beta^k \partial_k \alpha = -f(\alpha)\,\alpha^2(K - K_0)$$

"1+log" slicing condition: $f = 2/\alpha$ where $f(\alpha) > 0$ and $K_0 := K(t = 0)$

"Gamma-Driver" shift condition:

$$\partial_t \beta^i - \beta^j \partial_j \beta^i = \frac{3}{4}B^i,$$

$$\partial_t B^i - \beta^j \partial_j B^i = \partial_t \tilde{\Gamma}^i - \beta^j \partial_j \tilde{\Gamma}^i - \eta B^i$$

Mergers of two Hybrid Stars

One of the planned project deals with the numerical simulation of a hybrid star merger. During the merger process the mixed and probable also the pure quark phase is present in the inner core of the hypermassive compact star. The frequency spectrum of the emitted gravitational wave reflects some of the properties of the equation of state (K.Takami, L.Rezzolla, and L.Baiott, "Constraining the Equation of State of Neutron Stars from Binary Mergers", arXiv:1403.5672). Whether a Hadron-Quark phase transition is present during merger should be visible using gravitational wave detectors.
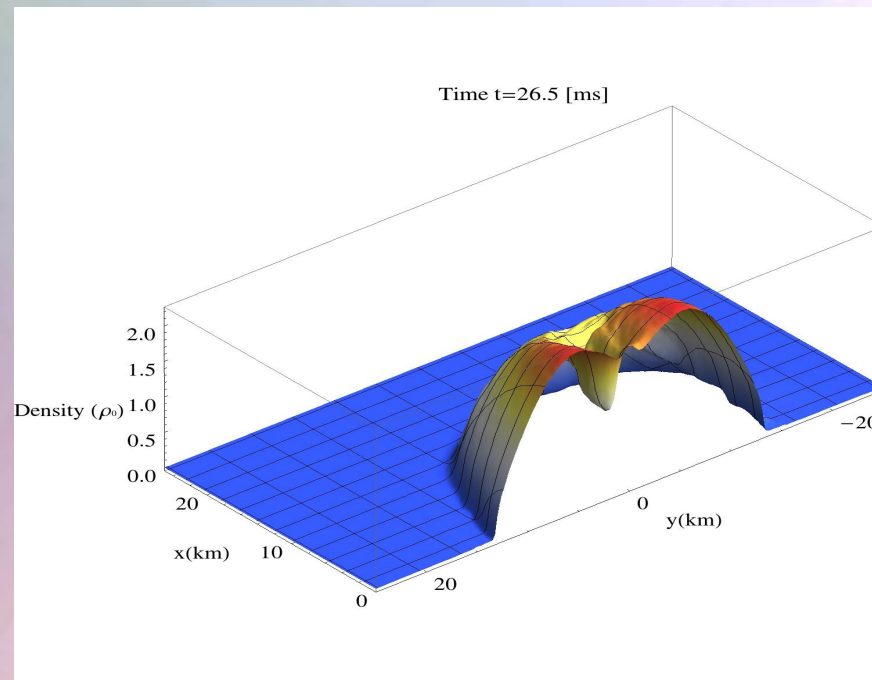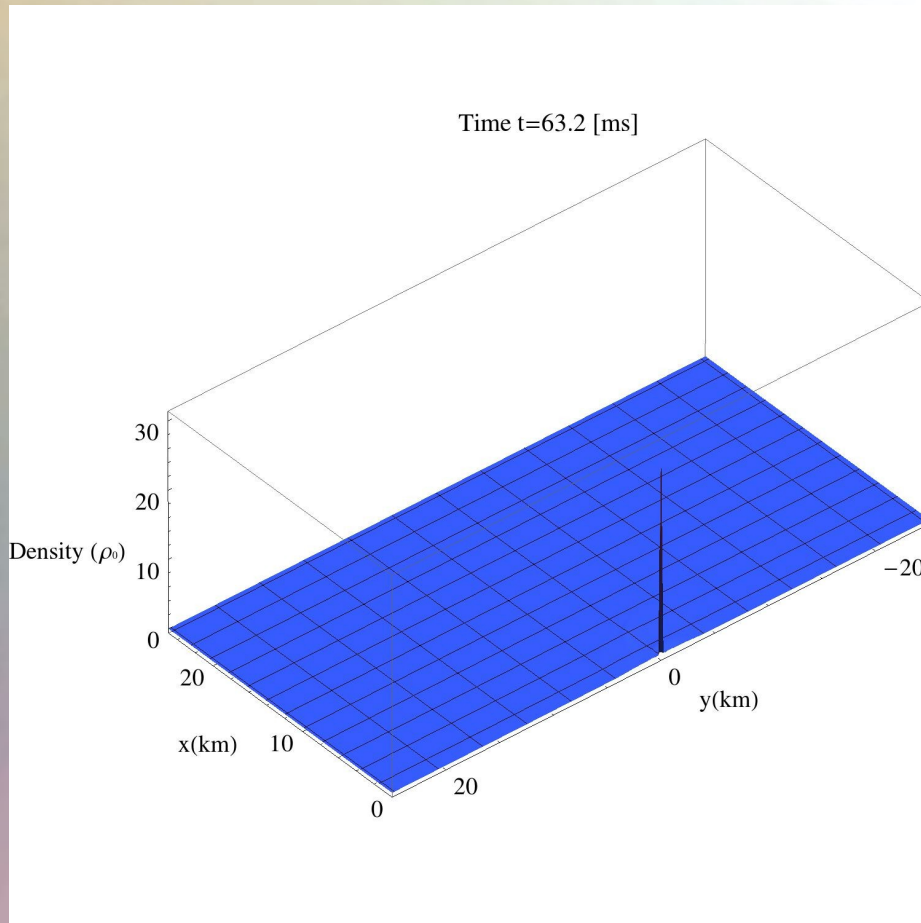

Simulations done by Kentaro Takami

Formation of the Black Hole
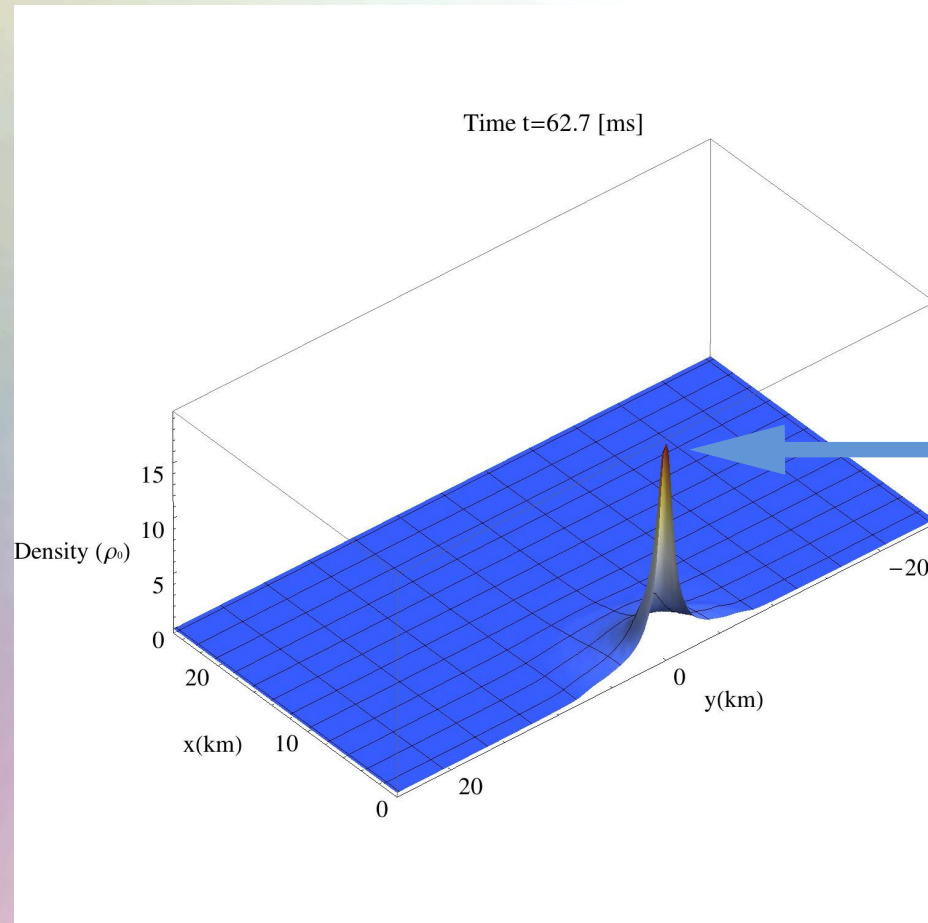
During the formation of the black hole, the star is mainly composed of quark matter

Formation of the Black Hole

The formation of the apparent and event horizon of the black hole confines the quark star macroscopically. Finally the colour charge of the deconfined, free quarks cannot be observed from outside.

Simulations done by Kentaro Takami